

# Renormalization group evolution of neutrino angles and masses

A Thesis

submitted to

Indian Institute of Science Education and Research Pune  
in partial fulfillment of the requirements for the  
BS-MS Dual Degree Programme

by

Ankur Panchal



Indian Institute of Science Education and Research Pune  
Dr. Homi Bhabha Road,  
Pashan, Pune 411008, INDIA.

May, 2021

Supervisor: Dr. Rahul Srivastava

© Ankur Panchal 2021

All rights reserved



# Certificate

This is to certify that this dissertation entitled Renormalization group evolution of neutrino angles and masses towards the partial fulfilment of the BS-MS dual degree programme at the Indian Institute of Science Education and Research, Pune represents study/work carried out by Ankur Panchal at Indian Institute of Science Education and Research under the supervision of Dr. Rahul Srivastava, Assistant Professor, Department of Physics, IISER Bhopal, during the academic year 2020-2021.



Dr. Rahul Srivastava

Committee:

Dr. Rahul Srivastava

Dr. Sachin Jain



This thesis is dedicated to my love for physics!



# Declaration

I hereby declare that the matter embodied in the report entitled Renormalization group evolution of neutrino angles and masses are the results of the work carried out by me at the Department of Physics, IISER Bhopal, Indian Institute of Science Education and Research, Pune, under the supervision of Dr. Rahul Srivastava and the same has not been submitted elsewhere for any other degree.

A handwritten signature in black ink that reads "Ankur Panchal". The signature is written in a cursive style with a horizontal line underlining the name.

Ankur Panchal



# Acknowledgments

I would like to express my sincere sense of gratitude to my supervisor, Dr. Rahul Srivastava for his guidance and support not only in the duration of the thesis but also during the pandemic times before the thesis work had started. I am also grateful to him, for his encouragement for making me think about and letting me explore the computational work with full freedom. It really helped me understand, the theoretical aspect of the project really well.

I am also thankful to Dinner session-chats with my dear friends at IISER Pune which kept my mind refreshed in this whole duration of 6 months I have been in IISER Pune.

I would also like to thank IISER Pune for allowing my stay at hostel during this tough time, to my TAC member Dr. Sachin Jain for all the recommendations and guidance that has led me to this project.

Last, but not the least, my parents for being a constant source of support and backing me and my capabilities.



# Abstract

Neutrinos are fundamental yet ill-understood particles in the standard model. The fact that they oscillate among each other is an indication towards non-zero masses of neutrinos. This highlights the limitations of the Standard Model of particle physics, which predicts massless neutrinos. Recent measurements of non-zero reactor angle has also opened up an opportunity for a wide variety of models and ansatz which try to explain neutrino masses' and angles' hierarchy. One key hypothesis is High Scale Mixing Unification (HSMU) hypothesis which tries to do the same by unifying mixing angles of quarks and leptons at GUT energy scale. In this thesis, we check the validity of HSMU predictions with the *recent* experimental bounds, as the measurements in recent years have highly increased in their precision. Furthermore, we also check an ansatz which demands less stringent requirements than HSMU, called Wolfenstein ansatz. It hypothesizes that the Wolfenstein parameterization structure in quarks' mixing matrix is duplicated in leptons' mixing matrix. We find that HSMU discards the possibility of neutrinos being Dirac particles and demands further analysis into Wolfenstein ansatz as it shows promising results



# Contents

<b>Abstract</b>	<b>xi</b>
<b>1 Introduction</b>	<b>5</b>
1.1 Background . . . . .	5
1.2 Open questions . . . . .	8
1.3 Motivation . . . . .	9
<b>2 Methods and tools</b>	<b>11</b>
2.1 Theoretical methods . . . . .	11
2.2 Computational tools . . . . .	15
<b>3 High Scale Mixing Unification (HSMU)</b>	<b>17</b>
3.1 General framework . . . . .	17
3.2 Predictions of HSMU framework . . . . .	18
3.3 HSMU Results: Mixing angles for Dirac and Majorana cases . . . . .	20
3.4 HSMU Results: Search for valid non-zero Majorana phases . . . . .	25
3.5 Conclusion from HSMU hypothesis . . . . .	29
<b>4 Wolfenstein Parameterization</b>	<b>31</b>

4.1	Background . . . . .	31
4.2	Results and discussions . . . . .	32
<b>5</b>	<b>Summary and outlook</b>	<b>43</b>
<b>A</b>	<b>Appendix</b>	<b>47</b>
A.1	PMNS matrix of Majorana neutrinos in mass diagonal basis <sup>[1]</sup> . . . . .	47
A.2	Extended SM Lagrangians used in REAP <sup>[2][3]</sup> . . . . .	47
A.3	RG running of $dim - 5$ operator ( $\kappa$ ) <sup>[4]</sup> . . . . .	48
A.4	RG running of Majorana phases <sup>[4]</sup> . . . . .	48
A.5	$\alpha, \beta$ variations for $\theta_{23}, \Delta m_{atm}^2$ and $m_{\beta\beta}$ in Wolfenstein ansatz . . . . .	48

# List of Figures

3.1	RG running of neutrino parameters . . . . .	19
3.2	Dirac case( $\delta = 0^\circ$ ): $\theta_{23}$ vs $\theta_{13}$ correlation . . . . .	21
3.3	Dirac case( $\delta \neq 0^\circ$ ): $\theta_{23}$ vs $\theta_{13}$ correlation . . . . .	22
3.4	Majorana case( $\varphi_1 = \varphi_2 = 0^\circ$ ): $\theta_{23}$ vs $\theta_{13}$ correlation . . . . .	24
3.5	Majorana case( $\varphi_1 = 120^\circ, \varphi_2 = 0^\circ$ ): $\theta_{23}$ vs $\theta_{13}$ correlation . . . . .	24
3.6	Majorana non-zero phases: $\Delta m_{atm}^2$ vs $m_{lightest}$ and $\Delta m_{sol}^2$ vs $m_{lightest}$ trend . . . . .	28
4.1	Wolfenstein parameterization: RG running of mixing angles for varying $\alpha, \beta$ . . . . .	33
4.2	Wolfenstein Parameterization: Low scale parameters vs $\lambda$ . . . . .	36



# List of Tables

3.1	Low scale Neutrino oscillation parameters data (N.O.) . . . . .	18
3.2	Low scale Quark oscillation parameters data . . . . .	18
3.3	Low scale neutrino parameters vs $\varphi_1, \varphi_2$ . . . . .	26
4.1	Qualitative trends of $\theta_{23}$ , $\Delta m_{atm}^2$ and $m_{\beta\beta}$ vs $\alpha, \beta$ for $\lambda = \lambda_{HSMU}$ for $\varphi_1 = 50^\circ$ , $\varphi_2 = 0^\circ$ and for $\varphi_1 = 50^\circ, \varphi_2 = 300^\circ$ . . . . .	39
4.2	Qualitative trends of $\theta_{23}$ , $\Delta m_{atm}^2$ and $m_{\beta\beta}$ vs $\alpha, \beta$ for $\lambda = \lambda_{HSMU}$ for $\varphi_1 = 200^\circ$ , $\varphi_2 = 300^\circ$ and for $\varphi_1 = 300^\circ, \varphi_2 = 50^\circ$ . . . . .	41
A.1	Quantitative trends of $\theta_{23}$ , $\Delta m_{atm}^2$ and $m_{\beta\beta}$ vs $\alpha, \beta$ for $\lambda = \lambda_{HSMU}$ . . . . .	49
A.2	Quantitative trends of $\theta_{23}$ , $\Delta m_{atm}^2$ and $m_{\beta\beta}$ vs $\alpha, \beta$ for $\lambda = \lambda_{HSMU}$ . . . . .	50



# Chapter 1

## Introduction

### 1.1 Background

#### 1.1.1 Neutrinos and the Standard Model

Neutrinos are uncharged leptons and fundamental particles in the standard model of particle physics. Just like charged leptons ( $e^-$ ,  $\mu^-$ ,  $\tau^-$ ), neutrinos have three flavour eigen states. In fact, every flavour of neutrino is in correspondence with the charged leptons. In a  $\beta$ -decay process, a neutron decays into a proton and an electron. But along with them one more particle is emitted, named electron-neutrino,  $\nu_e$  (an *anti*-neutrino, to be precise). Similarly, the neutrinos associated with  $\mu^-$  and  $\tau^-$  are called muon-neutrino ( $\nu_\mu$ ) and tau-neutrino ( $\nu_\tau$ ) respectively.

The Standard Model (SM) of particle physics had successfully combined most of the information about fundamental particles in nature. It was also backed up by experimental discoveries of W, Z bosons<sup>[5]</sup>, top quarks<sup>[6]</sup> and charm quarks<sup>[7][8]</sup>, as it had already predicted their existence and properties before they were observed. One of the many predictions of SM was also the fact that neutrinos are massless particles.

## 1.1.2 Neutrino Oscillations

As stated above, neutrinos come in three *flavours*. But in the late 1960s, an experiment which was supposed to measure the count of neutrinos emitted from the sun, showed a discrepancy in the count. The experimentally measured count was  $1/3^{\text{rd}}$  of what was predicted by the theory. This discrepancy is known as *the solar neutrino problem*<sup>[9]</sup>. The experiment was constantly performed for several years only to yield the same results. Finally it was confirmed in 2001<sup>[10]</sup> that the neutrinos of one flavour get transformed into neutrinos of the other flavours. That's why the discrepancy in the count. In the coming years, similar mixing of neutrino flavour eigen states were observed and confirmed by the experiments <sup>[11][12]</sup>. This phenomenon of neutrino flavour mixing is known as *neutrino oscillations*.

Now the problem is that the SM predicts that neutrinos are massless but in order to have oscillations possible, neutrinos must have mass eigenstates such that their flavours are mixture of these mass eigenstates. Neutrino oscillation experiments continue to show that neutrinos have non-degenerate masses and their flavour eigenstates mix with each other<sup>[13][14][15]</sup>. This means that there is some new physics beyond SM which should explain this. From here, starts the journey of physics beyond SM and many models are proposed to correct the SM in order to account for neutrino mixing phenomenon.

## 1.1.3 CKM and PMNS matrices

Mathematically, neutrino oscillations are seen as 'rotations' among flavour eigenstates and mass eigenstates. They are characterized by a matrix as particles are characterized by a column vector in the SM. Mixing of flavour eigenstates is also observed in quarks. The matrix explaining mixing in quarks is termed as CKM matrix<sup>†</sup> and that explaining mixing in leptons is termed as PMNS matrix

---

<sup>†</sup>CKM matrix is named after Cabibbo-Kobayashi-Maskawa

\*. They are as follows-

$$U_{CKM} = \begin{pmatrix} 0.97366 - 0.97384 & 0.2237 - 0.2253 & 0.00358 - 0.00406 \\ 0.217 - 0.225 & 0.976 - 0.998 & 0.0396 - 0.0424 \\ 0.0077 - 0.0083 & 0.0377 - 0.399 & 0.983 - 1.043 \end{pmatrix}^{[16]}$$

$$U_{PMNS} = \begin{pmatrix} 0.802 - 0.845 & 0.513 - 0.579 & 0.143 - 0.156 \\ 0.233 - 0.507 & 0.461 - 0.694 & 0.631 - 0.778 \\ 0.261 - 0.526 & 0.471 - 0.701 & 0.611 - 0.761 \end{pmatrix}^{[1]}$$

Each element  $U_{ij}$  corresponds to transitions of particles from flavour  $i$  to flavour  $j$ . The probabilities of these transitions are proportional to  $|U_{ij}|^2$ .  $U_{PMNS}$ , when acted on a mass eigenstate of neutrinos, returns the flavour eigenstate. Therefore, say, the neutrino  $\nu_e$  is observed as a mixture of three different neutrinos i.e.,  $\nu_e = U_{1j}\nu_j$ , where  $j = 1, 2, 3$ .

### 1.1.4 Oscillation parameters and parameterization

Usually any  $3 \times 3$  unitary matrix should be characterized by 9 independent degrees of freedom (3 angles and 6 phases). But in case of PMNS matrix, 5 of 6 phases are unphysical therefore we only have total 4 parameters (3 angles and 1 phase) to describe the PMNS matrix. The descriptions can be parameterized by various ways. A common parameterization is the *Standard parameterization*, given as follows-

$$U_{PMNS} = \begin{pmatrix} c_{12}c_{13} & s_{13}c_{13} & s_{13}e^{-i\delta_{CP}} \\ -s_{12}c_{23} - c_{12}s_{23}s_{13}e^{i\delta_{CP}} & c_{12}c_{23} - s_{12}s_{23}s_{13}e^{i\delta_{CP}} & s_{23}c_{13} \\ s_{12}s_{23} - c_{12}c_{23}s_{13}e^{i\delta_{CP}} & -c_{12}s_{23} - s_{12}c_{23}s_{13}e^{i\delta_{CP}} & c_{23}s_{13} \end{pmatrix}.$$

Three free parameter-angles are called neutrino mixing angles and are given by  $\theta_{12}$ ,  $\theta_{23}$  and  $\theta_{13}$ .  $c_{ij}$  and  $s_{ij}$  in the standard parameterization are  $\cos \theta_{ij}$  and  $\sin \theta_{ij}$  respectively.  $\delta_{CP}$  is the remaining free parameter of  $U_{PMNS}$  which describes Charge-Parity (CP) violations shown by leptons. These

---

\*PMNS matrix is named after Pontecorvo–Maki–Nakagawa–Sakata

4 parameters along with three neutrino masses are collectively termed as neutrino oscillation parameters. The similar parameterization in quarks, obtains mixing angles and  $\delta_{CP}$  for quarks. The experimentally measured values of quark and lepton mixing parameters are given in the Tables(3.1) and (3.2).

## 1.2 Open questions

Despite being postulated about a century ago, neutrinos still have characteristics which are very recently discovered or are ill-understood till this date. This is because neutrinos only interact through the weak force and it is supposedly a million times lighter than the otherwise lightest massive particle we know (the electron!). These features of neutrinos make it difficult to be detected and thus explain the lack of knowledge we have about them. A few open questions about neutrinos which are still unanswered are -

### (1) Are neutrinos their own anti-particles?

This question poses a possibility that neutrinos and anti-neutrinos are not distinct, just like photon. But unlike photon, neutrinos do have masses. To explain this, we need two more degrees of freedom which allows us to include particles like neutrinos which are massive as well as are their own anti-particles. These two physical degrees are called *Majorana phases* ( $\varphi_1$  and  $\varphi_2$ ) and such particles which are their own anti-particles are called *Majorana particles*. When neutrinos are considered Majorana particles, the standard parameterization includes  $\varphi_1$  and  $\varphi_2$  as shown in Appendix[A.1]. In other possibility where neutrinos and anti-neutrinos are distinct, they are called *Dirac particles*. The nature of neutrinos- whether Dirac or Majorana- is still not known.

## (2) What is the mass structure of different generations of neutrinos?

We know that quarks' masses are hierarchical in an increasing order with generations. But we still don't know whether neutrino masses have such a distinct hierarchy or they are quasi-degenerate<sup>†</sup>.

## (3) What is the mass hierarchy?

Even if they are quasi-degenerate or hierarchical like quarks, one must understand whether the hierarchy is normal, i.e.  $m_{\nu_1} > m_{\nu_2} > m_{\nu_3}$  or inverted, i.e.  $m_{\nu_1} > m_{\nu_3} > m_{\nu_2}$ . They are referred as normal order(N.O.) and inverse order(I.O.).

## (4) Why are quark mixing matrix and lepton mixing matrix so different?

From  $U_{CKM}$  and  $U_{PMNS}$  we can see that the mixing matrices of quarks and leptons are quite different. This translates to the fact that mixing happens differently among quark generations and lepton generations. We don't really understand why this happens to be what it is.

## 1.3 Motivation

In this thesis, we shall mainly focus on and try to contribute to the open questions (1) and (4). If possible, we will also try to check whether we can address the open questions (2) and (3).

To address the question(4), one of the hypothesis suggested in the literature is High Scale Mixing Unification (HSMU) hypothesis<sup>[17]</sup>. It tries to explain the difference in CKM and PMNS mixing parameters by stating that the current values are just an artefact of the energy scale at which these parameters are measured. HSMU hypothesis claims that the quark mixing angles and the lepton mixing angles would be the same at some high energy scale. It's the low energy scale at which we observe these angles to be so different. In other words, HSMU tries to *unify* the quark and lepton mixing angles at some high energy scale. Unification of two seemingly different phenomena is

---

<sup>†</sup>Quasi-degenerate masses refers to masses which are nearly(quasi) equal in values(degenerate.)

an age old idea in physics. Proposing unification theories has already helped us in the past in formulation of electroweak force, electromagnetism etc. This is the motivation behind HSMU hypothesis.

**The goal:** To verify this unification idea, we shall equate the quark mixing angles and the lepton mixing angles at some high energy scale and calculate the low energy scale values of the same. If the values that we theoretically calculate, match with the experimentally calculated values within some error range, we can be sure that HSMU holds true within our assumptions[[Chapter 3](#)]. In a nutshell, the goal is to calculate the values oscillation parameters at low energy scales within a certain error bound.

If HSMU does not hold true, i.e. if we can't bring these parameter values to be within their experimental ranges, we shall propose a slight variation of HSMU hypothesis [[Chapter 4](#)]. In this variation, we will lift the relatively stricter condition of mixing angles to be *exactly* equal at high energy scale and with the same goal we'll verify the variant hypothesis.

# Chapter 2

## Methods and tools

This chapter will discuss about the methods/procedure followed, both in theory and computation. It will also brief about pre-requisite knowledge needed in order to understand the next chapters and the computational tools used to perform those methods/procedures.

### 2.1 Theoretical methods

In order to realise HSMU, first we need to set up the theoretical background required. This includes some knowledge from QFT and Beyond Standard Model theories. Note that the theoretical methods discussed here are backed up by a strong mathematical backbone and methodical proofs. Discussing them in detail may result in deviation from the goals of the thesis. Hence the author will briefly touch upon the concepts and mention the necessary equations in the [Appendices](#).

### 2.1.1 Standard Model and its extensions

As SM fails to account for non-zero neutrino masses, we will use some extensions to SM as discussed below. These extensions are realised in the form of additional terms in the standard model Lagrangian.

**Grand Unified Theory (GUT):** This is a unification model of three coupling constants of the forces namely electromagnetic force, weak force and strong force. Unification of these coupling constants translates to unification of these fundamental forces in nature. The unification is said to have happened at a very large energy scale ( $10^{16}\text{GeV}$ ). We will refer to this energy scale as *GUT* scale and use it as the ‘high energy scale’ at which HSMU is realised.

**Minimal Supersymmetric Standard Model (MSSM):** Supersymmetry is a symmetry between SM fermions and bosons which hypothesizes a partner particle(“super-partner”) whose spin differs by  $1/2$  integer from every corresponding SM particle. MSSM model realizes this supersymmetry by assuming least number of new superpartner particles and hence the name *Minimal* supersymmetry. [2]. The superpartner particles are said to have *integrated out* (i.e., they aren’t detected) below their mass scale which is of the order of energy scale at which the supersymmetry breaks. This energy scale is referred as SuperSymmetry breaking scale (SUSY scale). It is roughly of the order of a few thousands of GeV. For this thesis, SUSY scale is taken to be 2000 GeV.

**Type-I seesaw mechanism(SS1)**[3]: This mechanism tries to explain why neutrinos have such low masses. In SSI mechanism, a large scale fermion singlet is coupled to electroweak doublet of massless neutrinos. This heavy mass is called the Majorana mass and its scale is called seesaw scale( $\mathcal{M}$ ), which is a way greater than the electroweak scale. This coupling is done through establishing Yukawa couplings to the Higgs scalar doublet. Spontaneous symmetry breaking in this case obtains mass eigenstates with very large( $\sim \mathcal{M}$ ) and very small( $\sim 1/\mathcal{M}$ ) eigenvalue. The very small mass is what we assign to the masses of neutrinos that we observe today which were

proposed to be massless in SM.

**Dimension-5 operator**<sup>[18]</sup>: The SM can be seen as an effective theory at low scale of a more fundamental theory at high scale. After right handed neutrinos are integrated out at seesaw scale, left handed neutrino masses at low scale are generated using a dimension 5 operator. Below seesaw scale, this operator is added to MSSM Lagrangian and once the SUSY breaks, it is added to the SM Lagrangian below SUSY scale.

The resultant Lagrangian combines MSSM with Type-I seesaw mechanism and  $dim - 5$  operator. Depending on which energy scale we are calculating oscillation parameters, the appropriate Lagrangian is chosen. The Lagrangian choice is discussed in the computational tools section(2.2.1).

## 2.1.2 Renormalization Group(RG) equations <sup>[4]</sup>

In high energy physics, RG equations are used to determine values of numerous variables at different energy scales. RG equations reduce the number of free parameters in a given system to its minimum. These parameters are input variables in RG equations as functions of energy scales. Constructing RG equations helps us determine the rate of change of these parameters as well their interactions among one another.

As the name suggests, HSMU requires values of several neutrino mixing parameters at *high* energy scales (GUT scale) and *low* energy scale,  $M_Z$  (energy scale corresponding to mass of Z boson). These parameters are namely, three neutrino mixing angles and three neutrino masses. The RG equations for the same are as follows-

$$\dot{\theta}_{12} = -\frac{C y_{\tau}^2}{32\pi^2} \sin(2\theta_{12}) s_{23}^2 \frac{|m_1 e^{i\phi_1} + m_2 e^{i\phi_2}|^2}{\Delta m_{sol}^2} + O(\theta_{13}) \quad (2.1)$$

$$\dot{\theta}_{13} = \frac{Cy_\tau^2}{32\pi^2} \sin(2\theta_{12}) \sin(2\theta_{23}) \frac{m_3}{\Delta m_{atm}^2 (1 + \zeta)} \times \left[ m_1 \cos(\varphi_1 - \delta) - (1 + \zeta)m_2 \cos(\varphi_2 - \delta) - \zeta m_3 \cos(\delta) \right] + O(\theta_{13}) \quad (2.2)$$

$$\dot{\theta}_{23} = -\frac{Cy_\tau^2}{32\pi^2} \sin 2\theta_{23} \frac{1}{\Delta m_{atm}^2} \left[ c_{12}^2 |m_2 e^{i\varphi_2} + m_3|^2 + s_{12}^2 \frac{m_2 e^{i\varphi_2} + m_3}{1 + \zeta} \right] + O(\theta_{13}) \quad (2.3)$$

$$\begin{aligned} 16\pi^2 \dot{m}_1 &= [\alpha + Cy_\tau^2 (2s_{12}^2 s_{23}^2 + F_1)] m_1 \\ 16\pi^2 \dot{m}_2 &= [\alpha + Cy_\tau^2 (2c_{12}^2 s_{23}^2 + F_2)] m_2 \\ 16\pi^2 \dot{m}_3 &= [\alpha + 2Cy_\tau^2 c_{13}^2 c_{23}^2] m_3 \end{aligned} \quad (2.4)$$

$$\begin{aligned} 8\pi^2 (\Delta m_{sol}^2) &= \alpha \Delta m_{sol}^2 + Cy_\tau^2 [2s_{23}^2 (m_2^2 c_{12}^2 - m_1^2 s_{12}^2) + F_{sol}] \\ 8\pi^2 (\Delta m_{atm}^2) &= \alpha \Delta m_{atm}^2 + Cy_\tau^2 [2m_3^2 s_{13}^2 c_{23}^2 - 2m_2^2 c_{12}^2 s_{23}^2 + F_{atm}] \end{aligned} \quad (2.5)$$

where  $\dot{\theta}$ ,  $\dot{m}$  and  $\dot{m}^2$  represent  $\frac{d\theta}{dt}$ ,  $\frac{dm}{dt}$  and  $\frac{dm^2}{dt}$  respectively

$t = \ln\left(\frac{\mu}{\mu_0}\right)$ , where  $\mu$  is the variable energy scale and  $\mu_0$  is the initial energy scale from where RG running starts.

$$\Delta m_{sol}^2 = (m_2^2 - m_1^2) \ \& \ \Delta m_{atm}^2 = (m_3^2 - m_2^2)$$

$s_{ij}$  and  $c_{ij}$  are  $\sin \theta_{ij}$  and  $\cos \theta_{ij}$  respectively.

$C = -3/2$  for MSSM and  $C = 1$  for SM.

$$\zeta = \frac{\Delta m_{sol}^2}{\Delta m_{atm}^2}$$

$y_\tau$  is 3<sup>rd</sup> generation element of Yukawa coupling matrix  $Y_e$ .

$$F_1 = -s_{13} \sin 2\theta_{12} \sin 2\theta_{23} \cos \delta + 2s_{13}^2 c_{12}^2 c_{23}^2$$

$$F_2 = s_{13} \sin 2\theta_{12} \sin 2\theta_{23} \cos \delta + 2s_{13}^2 s_{12}^2 c_{23}^2$$

$$F_{sol} = (m_1^2 + m_2^2) s_{13} \sin 2\theta_{12} \sin 2\theta_{23} \cos \delta + 2s_{13}^2 c_{23}^2 (m_2^2 s_{12}^2 - m_1^2 c_{12}^2)$$

$$F_{atm} = -m_2^2 s_{13} \sin 2\theta_{12} \sin 2\theta_{23} \cos \delta - 2m_2^2 s_{12}^2 s_{13}^2 c_{23}^2$$

Note that we will be using mass squared differences  $\Delta m_{sol}^2$  and  $\Delta m_{atm}^2$  instead of individual masses  $m_1, m_2, m_3$ . This is because massiveness of neutrinos is known to us only through neutrino oscilla-

tion experiments. Probability of Neutrino oscillation between  $\nu_i$  and  $\nu_j$  depends on  $(m_i^2 - m_j^2)$  and that's exactly what we measure in experiments. Even though there are three possible oscillations we consider only two mass squared differences because the remaining one is redundant. The  $M_Z$  scale values of three neutrino mixing angles and the two mass squared differences are what we shall refer to as *low scale parameters* from now onward.

## 2.2 Computational tools

To implement the plan, all the computations were done using Wolfram Mathematica v12.0. *Renormalization Group Evolution of Angles & Phases* (REAP) and *MixingParametersTools* (MPT) are the packages used, both v1.9.3.

### 2.2.1 Renormalization Group Evolution of Angles & Phases (REAP)

REAP package has particle physics models- Standard Model(SM), Minimal Supersymmetric Standard Model (MSSM) and Two Higgs Doublet Model (2HDM) already loaded in it. These models can be implemented with *dimension-5 neutrino mass operator* and *type-I seesaw mechanism*. REAP also helps to solve the RG equations and thus obtain us relevant parameters at desired energy scales, for example mass matrices, gauge couplings, etc. While running from GUT scale to  $M_Z$  scale the models are loaded in the following manner-

- Below GUT scale till seesaw scale: MSSM with type-I seesaw mechanism
- Below seesaw scale till SUSY breaking scale: MSSM with dimension-5 neutrino mass operator
- Below SUSY breaking scale till  $M_Z$  scale: SM with dimension-5 neutrino mass operator

The package gives options to add the models with or without right handed neutrinos. They are integrated out once we are at energy scales below their mass threshold. One can also load the

models with considerations of neutrinos being Dirac particles or Majorana particles. A model (SM/MSSM) is provided with some input values specific to that model. For the work in this thesis, following inputs are given as the initial values before RG running-

- $M_Z$  scale = 91.1876 GeV
- GUT scale =  $2 \times 10^{16}$  GeV
- $\tan\beta = 55$  ( $\beta$  is the ratio of expectation values of Higgs doublets in 2HDM)
- SUSY cutoff scale = 2000 GeV
- Values of gauge coupling constants
  - Higgs coupling = 0.4615 (at  $M_Z$  scale) & 0.7013 (at GUT scale)
  - Weak coupling = 0.6519 (at  $M_Z$  scale) & 0.6904 (at GUT scale)
  - Strong coupling = 1.2198 (at  $M_Z$  scale) & 0.6928 (at GUT scale)
- Quark mixing parameters at  $M_Z$  scale (mixing angles and Yukawa matrix elements) [From table(3.2) and section(1.1.3)]
- Lepton Yukawa matrix elements at  $M_Z$  scale [From table(3.1) and section(1.1.3)]
- Quark and Lepton CP violation phases
- Self Higgs coupling ( $\lambda$ ) = 0.1291
- Higgs ground state VEV( $v$ ) = 246 GeV

These models have variants which can calculate all values up to 1-loop or 2-loop corrections. Calculations concerning this thesis are done with 2-Loop variants of SM and MSSM.

### 2.2.2 MixingParameterTools (MPT)

MPT package allows us to find mass eigenvalues, mixing angles and phases from mass matrix of neutrinos. Given high scale values of mixing angles, masses and CP violation phase, a neutrino mass matrix ( $Y_\nu$ ) is calculated at the low energy scale using REAP. MPT extracts values of low scale masses, mixing angles and phases. These values and few more quantities generated by these values, are cross-checked with the already established experimental values within some error bound. We consider values of low scale parameters within  $3 - \sigma$  experimental range. The ranges are mentioned in the next chapter[Table(3.1)].

# Chapter 3

## High Scale Mixing Unification (HSMU)

Equipped with all the computational tools and theoretical knowledge, we are ready to dive into the actual application of HSMU.

### 3.1 General framework

We initialize the process with CKM matrix elements, i.e. quarks parameters[see Table(3.2)]. Gauge couplings, Higgs parameters, quarks' CP violation phase( $\delta_q$ ) are also provided along with these parameters as given in 2.2.1. Then we use REAP to run the CKM parameters using RG equations from  $M_Z$  scale to  $GUT$  scale. Using MPT, we extract the quarks mixing angles at  $GUT$  scale. This process is called *Bottom-Up running of CKM parameters*, as the RG evolution starts from lower(bottom) scale and ends at higher(Up) scale.

Now according to HSMU we take the high scale quark mixing angles to be **equal** to high scale neutrino mixing angles. To evaluate all the neutrino parameters at  $M_Z$  scale, we will also need neutrino masses at  $GUT$  scale. These are independent parameters and hence, are manually provided at  $GUT$  scale. With mixing angles(from CKM angles) and masses(independent) available at  $GUT$  scale, we can use them as an input to evaluate neutrino mass matrix at  $M_Z$  scale using REAP again.

This time we have to run the RG equations from  $GUT$ (top) scale to  $M_Z$ (down) scale and thus, it's called *Top-Down running of neutrino parameters*. The neutrino mixing angles and masses are obtained at  $M_Z$  scale using MPT package.

## 3.2 Predictions of HSMU framework

### 3.2.1 Mass ordering and degeneracy

All three angles( $\theta_{12}, \theta_{23}, \theta_{13}$ ) and two mass squared differences ( $\Delta m_{sol}^2, \Delta m_{atm}^2$ ) at low scale are compared to their experimentally measured values upto  $3 - \sigma$  precision[mentioned in Table(3.1)].

Table 3.1: Low scale Neutrino oscillation parameters data (N.O.)<sup>[19]</sup> [20]

Oscillation parameters	3- $\sigma$ range	Best fit values
$\theta_{12}$	31.37° - 37.46°	34.33°
$\theta_{13}$	8.16° - 8.94°	8.58°
$\theta_{23}$	41.61° - 51.30°	48.79°
$\Delta m_{atm}^2$	$2.39 \times 10^{-3} - 2.57 \times 10^{-3} eV^2$	$2.49 \times 10^{-3} eV^2$
$\Delta m_{sol}^2$	$6.94 \times 10^{-5} - 8.14 \times 10^{-5} eV^2$	$7.50 \times 10^{-5} eV^2$

Table 3.2: Low scale Quark oscillation parameters data<sup>[21]</sup>  $\delta_q$  is CP violation phase of quarks.

Oscillation parameters	1- $\sigma$ range	Best fit values
$\theta_{q12}$	13.0629° - 13.1193°	13.0911°
$\theta_{q13}$	0.2017° - 0.2131°	0.2068°
$\theta_{q23}$	2.2879° - 2.3876°	2.3228°
$\delta_q$	66.06° - 71.10°	68.53°

In bottom-up RG running, quark parameters don't change much in their values. Hence when we implement HSMU hypothesis by equating  $GUT$  scale quark mixing angles to  $GUT$  scale neutrino angles, the top-down running of  $\theta_{23}$  has to be magnified by a large amount (from 2° to 48°). This

magnification, called *Radiative magnification*, is thus needed in order to realise HSMU hypothesis. This is the reason to assume normal ordering(N.O.) in neutrino masses, as the values which are calculated assuming inverted ordering(I.O.) don't produce the desired radiative magnification. Thus HSMU hypothesis, if validated to be true, suggests N.O. in neutrino masses.

Furthermore, from Eq.(2.1), (2.2) and (2.3) it can be noticed that  $|\dot{\theta}| \propto (\Delta m^2)^{-1}$ . This means that more the change in  $\theta$ s, less the mass squared differences at that particular energy scale. Thus radiative magnification of angles in HSMU in top-down RG running is suggestive of quasi-degenerate masses of neutrinos. These predictions (radiative magnification and quasi-degenerate masses) are to be verified by computations, which is discussed the next.

### 3.2.2 Computational verifications

Using the initial values of all parameters as mentioned previously, the REAP and MPT packages we can finally implement RG running. A typical RG running of neutrino parameters are shown below.

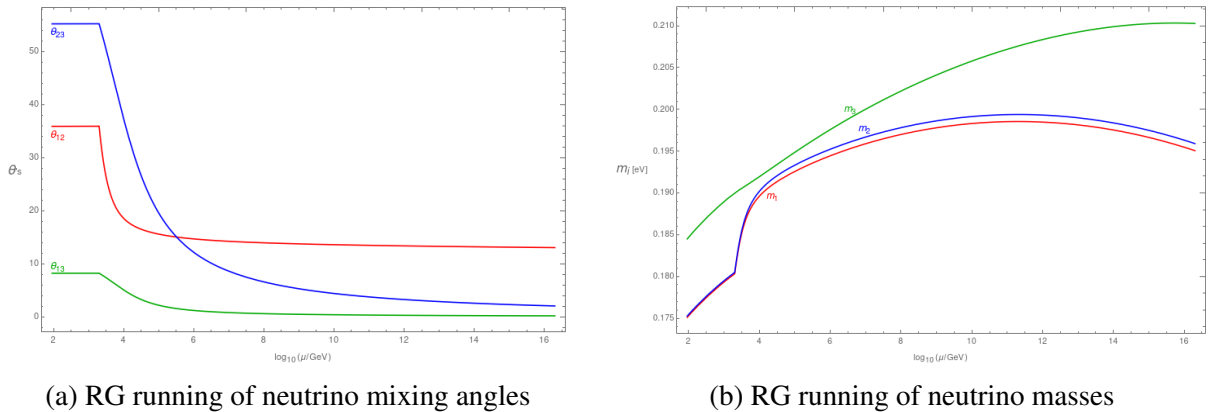


Figure 3.1: Neutrino parameters vs logarithmic energy scale.

Without loss of generality, we have chosen a case where the graphs represent Dirac nature of neutrinos and the CP violation phase of neutrinos at *GUT* scale is taken to be equal to that of quarks at *GUT* scale. As discussed in the general framework, the independent parameters that we can choose by ourselves, are the neutrino masses at *GUT* scale. From Fig.(3.1a), it can be seen that angles at low( $M_Z$ ) scale are significantly magnified in values. Especially, radiative magnification

in  $\theta_{23}$  is the largest just as expected from the predictions. From Fig.(3.1b), it is clear that masses at  $M_Z$  scale are also quasi-degenerate in values. The maximum difference between any pair of mass is 0.01 eV, which is quite small.

With these successful predictions, we move on to check whether we can find a suitable set of  $GUT$  scale masses(the independent parameters) so that the low scale mixing parameters lie within their valid ranges as mentioned in Table(3.1).

### 3.3 HSMU Results: Mixing angles for Dirac and Majorana cases

Along with  $GUT$  scale masses, there are multiple degrees of freedom which we can account for, to analyse the RG evolution of parameters. We look into a few of the possible cases which can be formed with these degrees of freedom. First of all, we check whether neutrinos are Dirac particles or Majorana particles. Furthermore, one can also check the effects of CP violation phase and varying Majorana phases [discussed in section(3.4)]. A systematic approach would be to have all the mixing angles inside their  $3 - \sigma$  ranges by broadly varying the high scale masses. Then, we further try to fine-tune the high scale masses such that mass squared differences can also come inside their valid ranges.

#### 3.3.1 Dirac case

We start with assuming Dirac nature for neutrinos. This translates to loading SM and MSSM models with Dirac case option. In this case, we consider two sub-cases- one when neutrinos are CP violating ( $\delta \neq 0$ ) and the other when they are CP conserving ( $\delta = 0$ ). In order to effectively understand whether we can bring in all the mixing angles, we will see effects of low scale  $\theta_{12}$  value on the correlation between low scale  $\theta_{23}$  and  $\theta_{13}$ . This way we can be sure of whether there exists a parameter space for which all three angles are brought inside their  $3 - \sigma$  ranges.

(i) CP conserving neutrinos ( $\delta = 0$ )

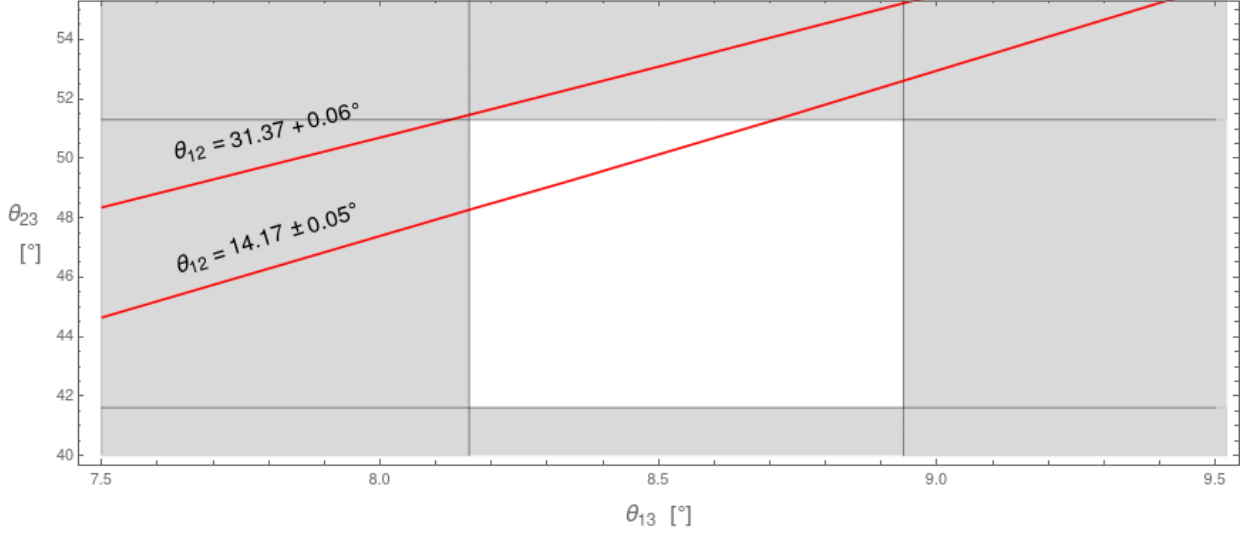


Figure 3.2:  $\theta_{23}$  vs  $\theta_{13}$  with  $\delta = 0^\circ$ . The correlation is a straight line. Different straight lines would correspond to different  $\theta_{12}$ . The shaded regions are out of  $3 - \sigma$  ranges of  $\theta_{23}$  and  $\theta_{13}$ .

Fig.(3.2) shows the correlation between  $\theta_{23}$  and  $\theta_{13}$  at low scale. As the gray shaded region corresponds to experimentally forbidden values of  $\theta_{23}$  and  $\theta_{13}$ , the line passing through the white rectangular region corresponds to allowed values of both  $\theta_{23}$  and  $\theta_{13}$  simultaneously. But for the same line,  $\theta_{12}$  is  $14.17^\circ$  which is invalid low scale value for  $\theta_{12}$ . Thus this line can be discarded as we can not have all three angles' low scale values within their  $3 - \sigma$  ranges. When  $\theta_{12}$  is varied the linear correlation function moves with respect to the allowed (white) region. If  $\theta_{12}$  is increased the line moves to the top-left corner of the allowed region, indicating that for those values of  $\theta_{12}$  we can not have  $\theta_{23}$  and  $\theta_{13}$  within their  $3 - \sigma$  ranges. We can see that for the minimum valid value of  $\theta_{12}$  the line is completely outside the allowed region, which tells us that we will never have a suitable value-space of mixing angles for which all of them lie within their valid ranges. We can claim this because RG equations are monotonous functions of  $\theta_{12}$  and therefore any further increment in the value of  $\theta_{12}$  will move the correlation even further away from the allowed region.

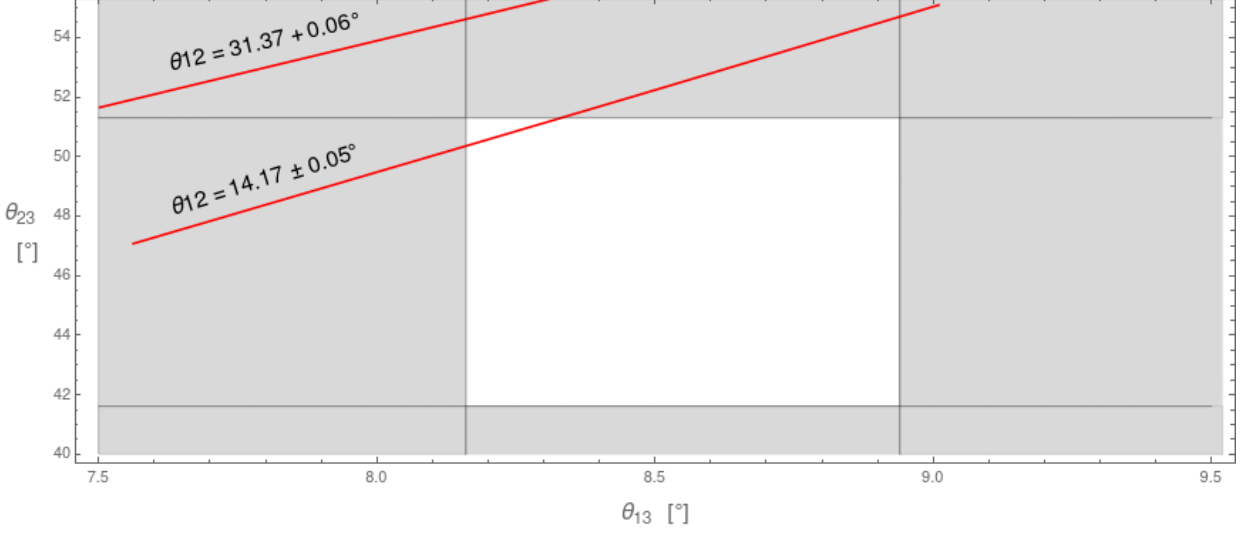


Figure 3.3:  $\theta_{23}$  vs  $\theta_{13}$  with  $\delta \neq 0^\circ$ . The correlation is a straight line. Different straight lines would correspond to different  $\theta_{12}$ . The shaded regions are out of  $3 - \sigma$  ranges of  $\theta_{23}$  and  $\theta_{13}$ .

### (ii) CP violating neutrinos ( $\delta \neq 0$ )

In this case we take  $\delta$  at high scale to be equal to quarks' CP violating phase at high scale. Running down from  $GUT$  scale to  $M_Z$  scale, we still can't have all three angles inside their  $3 - \sigma$  ranges, as can be seen from Fig.(3.3). The result remains the same as in CP conserving case. Valid values of  $\theta_{12}$  will correspond to  $\theta_{23}$  vs  $\theta_{13}$  correlation functions lying completely outside the allowed region. Thus, when we assumed neutrinos to be Dirac particles neither CP conserving nor CP violating case allows us to have all mixing angles within their  $3 - \sigma$  range. Note that we need not check mass square differences' low scale values as angles will anyway be not within desired range.

### 3.3.2 Majorana case

In this case we consider neutrinos to be Majorana particles, i.e., they are their own anti-particles. We have two more degrees of freedom with Majorana nature of neutrinos- Two Majorana phases ( $\varphi_1$  and  $\varphi_2$ ). With them we can form two sub-cases, one when Majorana phases are zero and the other when they are non-zero. Note that we are not introducing the effects of  $\delta$ . For simplicity,

we are fixing  $\delta$  to be equal to  $\delta_q$  at high scale. In addition to five low scale ( $M_Z$ ) parameters of neutrino oscillation, we will also check one more quantity at low scale, called *effective Majorana mass* ( $m_{\beta\beta}$ ).

### Neutrinoless double beta ( $0\nu\beta\beta$ ) decay [20] & Effective Majorana mass ( $m_{\beta\beta}$ )

A double beta decay is a process where two neutrons are simultaneously decaying to form two protons by emitting two anti-neutrinos. Now, if the neutrinos are Majorana particles, anti-neutrinos and neutrinos would be the same. Such a double beta decay process annihilate the neutrino-antineutrino pair and we wouldn't obtain neutrinos as emitted particles at the end. Only electrons would be observed and neutrinos will behave like a virtual particle in the process. A decay rate of such a process  $\Gamma \propto |m_{\beta\beta}|^2$ . The  $m_{\beta\beta}$ , called the effective Majorana mass, is experimentally measured in the double beta process. The most stringent upper bound range on  $m_{\beta\beta}$  is set by KamLAND-Zen experiment and its value ranges from 0.065 eV to 0.165 eV [20]. In this thesis we will use the looser end of its upper bound, i.e., we will also check whether low scale value of  $m_{\beta\beta}$  is  $< 0.165$  eV.

#### (i) Majorana phases, $\varphi_1 = \varphi_2 = 0^\circ$

Note that this case [Fig.(3.4)] is similar to Dirac case with non-zero  $\delta$ . Because in both the cases  $\delta$  is equal to  $\delta_q$  at  $GUT$  scale and there was no Majorana phases in Dirac case. Although, the difference between them lies in the high scale masses that are not shown here. The reason for no necessity to look into masses is the same as before, that all three angles themselves couldn't not be brought into their  $3 - \sigma$  range. So this case can also be discarded to hold true.

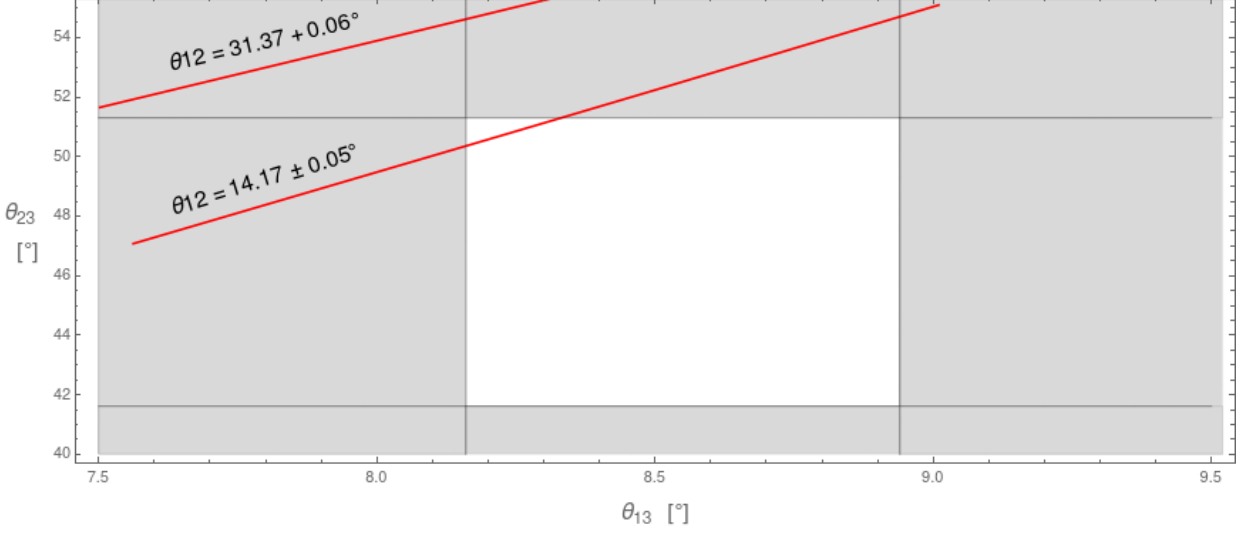


Figure 3.4:  $\theta_{23}$  vs  $\theta_{13}$  with  $\varphi_1 = \varphi_2 = 0^\circ$ . The correlation is a straight line. Different straight lines would correspond to different  $\theta_{12}$ . The shaded regions are out of  $3 - \sigma$  ranges of  $\theta_{23}$  and  $\theta_{13}$ .

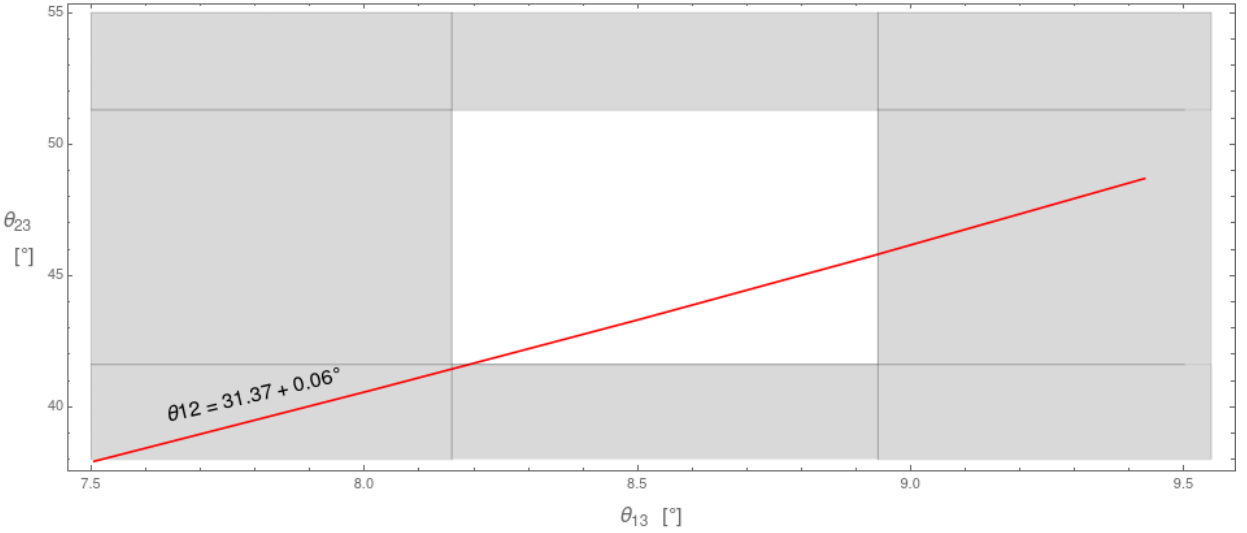


Figure 3.5:  $\theta_{23}$  vs  $\theta_{13}$  with  $\varphi_1 = 120^\circ$ ,  $\varphi_2 = 30^\circ$ . The correlation is a straight line. Different straight lines would correspond to different  $\theta_{12}$ . The shaded regions are out of  $3 - \sigma$  ranges of  $\theta_{23}$  and  $\theta_{13}$ .

**(ii) Non-zero Majorana phases,  $\varphi_1 \neq 0, \varphi_2 \neq 0$**

We first find arbitrary non-zero Majorana phases to check whether all  $\theta$ s can be brought inside their valid ranges. For  $\varphi_1 = 120^\circ$  and  $\varphi_2 = 30^\circ$  the correlation of  $\theta_{23}$  vs  $\theta_{13}$  is as shown in Fig.(3.5)

Finally, for the minimum value of  $\theta_{12}$  we obtained the correlation line function to be inside the

allowed region formed by  $\theta_{23}$  and  $\theta_{13}$ . As previously seen, increasing  $\theta_{12}$  will shift the function upwards. But in spite of that we would safely have a valid  $\theta_{23}$  vs  $\theta_{13}$  space for which  $\theta_{12}$  can be inside the allowed region. That means, for this pair of  $\varphi_1$ ,  $\varphi_2$  we could bring in all the mixing angles within their  $3 - \sigma$  range. Since this pair of Majorana phases was chosen arbitrarily, we dug deep into understanding the effects of Majorana phases on low scale parameters, which is discussed in the next section.

### 3.4 HSMU Results: Search for valid non-zero Majorana phases

Till now, it is established that for a pair of non-zero Majorana phases, we can bring in all neutrino angles inside their  $3 - \sigma$  ranges. We now move on to find Majorana phases-  $\varphi_1$ ,  $\varphi_2$  such that the mass square differences ( $\Delta m_{atm}^2$  and  $\Delta m_{sol}^2$ ) and  $m_{\beta\beta}$  are also inside their respective  $3 - \sigma$  ranges. Instead of scanning through randomly generated values of  $\varphi_1$ ,  $\varphi_2$  from the whole  $[0, 2\pi]$  range, we manually choose some discrete values of them. This is because it's very less probable that we get a suitable value set for  $GUT$  scale  $\varphi$ 's if we choose randomly. We fix one  $\varphi$  and record the effect of other  $\varphi$  on the number of low scale parameters that can be brought inside their  $3 - \sigma$  ranges as well as on  $\Delta m_{atm}^2$  &  $\Delta m_{sol}^2$ .

#### 3.4.1 Effect of $\varphi$ 's on $\Delta m_{atm}^2$ and $\Delta m_{sol}^2$ :

We can carry out our search with or without low scale  $m_{\beta\beta}$  constraint. Table[3.3] shows whether the low scale parameters are within their  $3 - \sigma$  ranges for each pair of  $\varphi_1$ ,  $\varphi_2$  examined. From Table[3.3(a)], it is clear that with  $m_{\beta\beta}$  constraint applied, we can not bring in  $\Delta m_{atm}^2$  (along with all 3 angles) inside its valid range for any combination of high scale  $\varphi$ 's. It is to be noted that in spite of examining only a few discrete values of  $\varphi$ 's, we can claim this for the whole range  $[0, 2\pi]$  because  $\Delta m_{atm}^2$  varies monotonously and continuously with  $\varphi$ 's. We can bring in  $\Delta m_{atm}^2$  by varying masses of neutrinos at the  $GUT$  scale but only when the low scale  $m_{\beta\beta}$  constraint is relaxed.

$\varphi_1(^{\circ})$	$\varphi_2(^{\circ})$	$\theta_{12}$	$\theta_{13}$	$\theta_{23}$	$\Delta m_{sol}^2$	$\Delta m_{atm}^2$
50	0	✓	✓	✓	✓	-
100	0	✓	✓	✓	-	-
200	0	✓	✓	✓	-	-
300	0	✓	-	✓	✓	-
0	50	✓	-	✓	✓	-
50	50	✓	-	✓	✓	-
100	50	✓	✓	✓	-	-
200	50	✓	-	✓	-	-
300	50	✓	✓	✓	✓	-
0	100	✓	-	✓	✓	-
50	100	✓	-	✓	✓	-
100	100	✓	✓	✓	-	-
200	100	✓	-	✓	-	-
300	100	✓	-	✓	✓	-
0	200	✓	-	-	-	-
50	200	✓	-	✓	✓	-
100	200	✓	-	✓	-	-
200	200	✓	-	✓	-	-
300	200	✓	✓	-	-	✓
0	300	✓	-	✓	✓	-
50	300	✓	✓	✓	✓	-
100	300	✓	✓	✓	-	-
200	300	✓	✓	✓	✓	-
300	300	✓	-	✓	✓	-

(a)

$\varphi_1(^{\circ})$	$\varphi_2(^{\circ})$	$\theta_{12}$	$\theta_{13}$	$\theta_{23}$	$\Delta m_{sol}^2$	$\Delta m_{atm}^2$
50	0	✓	✓	✓	Only one	
100	0	✓	✓	✓	Only one	
200	0	✓	✓	✓	Only one	
300	0	✓	Only one		Only one	
0	50	✓	Only one		Only one	
50	50	✓	Only one		Only one	
100	50	✓	✓	✓	Only one	
200	50	✓	Only one		Only one	
300	50	✓	✓	✓	Only one	
0	100	✓	Only one		Only one	
50	100	✓	Only one		Only one	
100	100	✓	✓	✓	Only one	
200	100	✓	Only one		Only one	
300	100	✓	Only one		Only one	
0	200	✓	Only one		Only one	
50	200	✓	Only one		Only one	
100	200	✓	Only one		Only one	
200	200	✓	Only one		Only one	
300	200	✓	Only one		Only one	
0	300	✓	Only one		Only one	
50	300	✓	✓	✓	Only one	
100	300	✓	✓	✓	Only one	
200	300	✓	✓	✓	Only one	
300	300	✓	Only one		Only one	

(b)

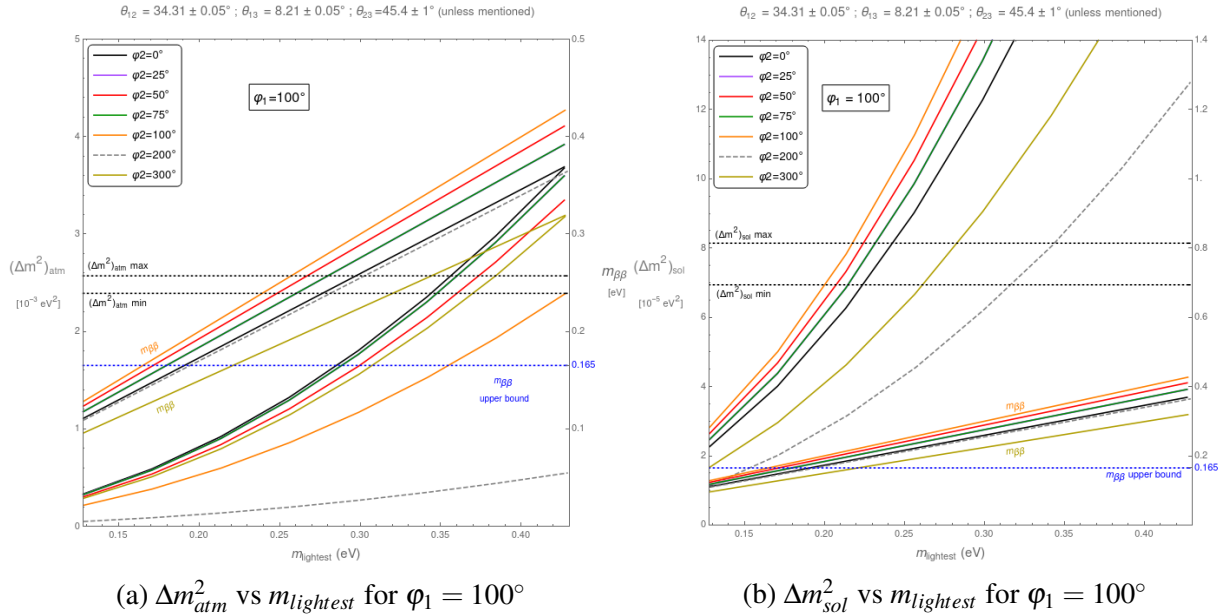
Table 3.3: '✓' represents the fact that the corresponding parameter has a valid(within experimental 3- $\sigma$  range) value. (a)  $m_{\beta\beta}$  is inside its bounds for ALL combinations of  $\varphi_1, \varphi_2$ . (b)  $m_{\beta\beta}$  may or may NOT be inside its bounds.

### 3.4.2 The trend of $\Delta m_{atm}^2, \Delta m_{sol}^2$ and $m_{\beta\beta}$ vs $\varphi$ 's & $m_{lightest}$

Neutrino masses(at large scale) play a large role changing the low scale values of  $\Delta m_{atm}^2, \Delta m_{sol}^2$  and  $m_{\beta\beta}$ . It can be insightful to understand the extent by which we can't bring  $\Delta m_{atm}^2, \Delta m_{sol}^2$  and  $m_{\beta\beta}$  in their valid ranges. This extent can be analyzed by plotting them against one of the masses. We choose the lightest neutrino mass ( $m_{lightest} = m_1$ ) for the same. Fig.(3.6) shows the trend of  $\Delta m_{atm}^2, \Delta m_{sol}^2$  and  $m_{\beta\beta}$  plotted against  $m_{lightest}$  for all the variations of  $\varphi_1, \varphi_2$  mentioned in the

table[3.3].

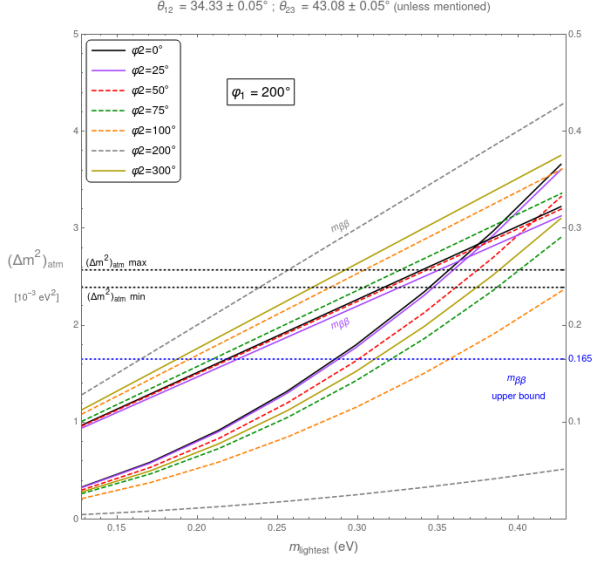
In these figures we can notice the region on  $m_{lightest}$  axis where the  $m_{\beta\beta}$  lines are below its upper bound. The curved lines for those  $m_{\beta\beta}$  values can be inside the bounded range, above the range or below the range. Comparing graphs for  $\Delta m_{sol}^2$  and  $\Delta m_{atm}^2$  side by side one can estimate whether, for a particular set of  $\varphi$ 's or for a particular value of  $m_{lightest}$ ,  $\Delta m_{sol}^2$  or  $\Delta m_{atm}^2$  are above or below their corresponding ranges. This can help us choose such a data set, where we can choose to either keep  $\Delta m_{sol}^2$  or  $\Delta m_{atm}^2$  outside the range and then determine how we can bring in the fifth low scale parameter value inside its  $3-\sigma$  range.



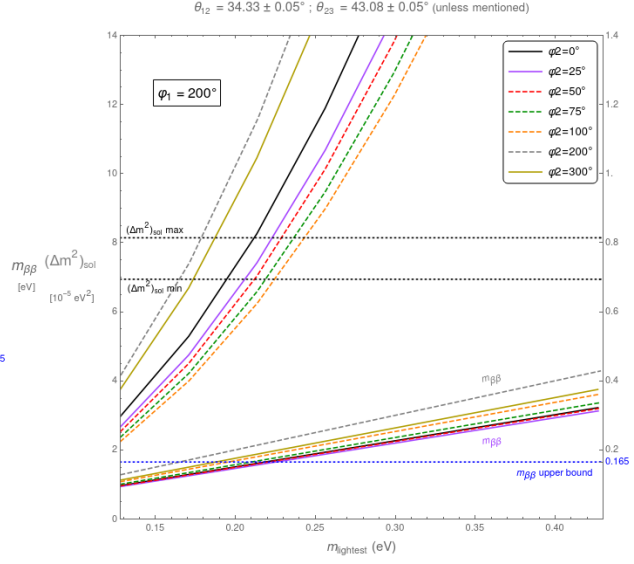
### Analysis of the trends

Consider Fig.(3.6a) and Fig.(3.6b). In both the figures, none of  $\Delta m^2$ 's lie in their bounded ranges for a valid region for  $m_{lightest}$  values for which  $m_{\beta\beta}$  is below its upper bound. In conclusion, for this set of  $\varphi$ 's, we can NOT have both  $\Delta m_{sol}^2$  and  $\Delta m_{atm}^2$  inside their  $3-\sigma$  ranges satisfying the  $m_{\beta\beta}$  upper bound and thus we can move on to the next  $\varphi_1$ 's values ( $\varphi_1 = 200^\circ, 300^\circ$ ).

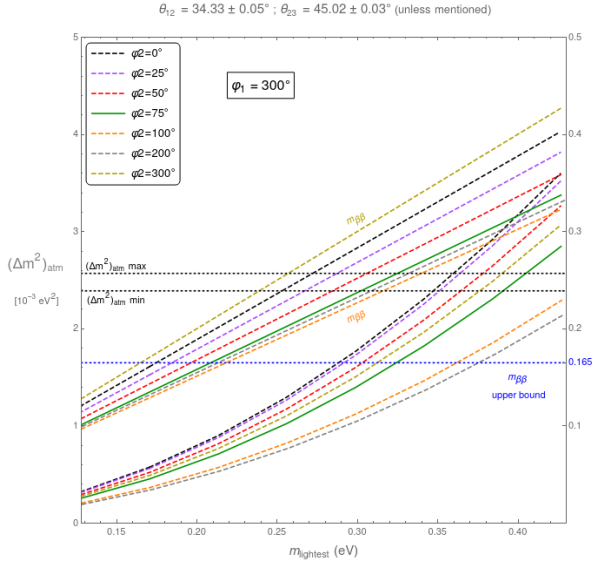
From Fig.(3.6c), we understand that there are only 3 combinations of  $\varphi_1$  and  $\varphi_2$  for which all three neutrino angles can be brought in. But for valid  $m_{\beta\beta}$  values, all three solid curved lines ( $\Delta m_{atm}^2$ )



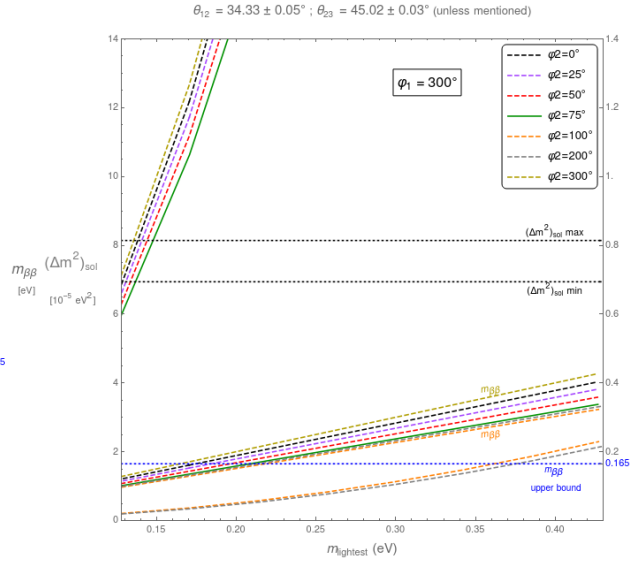
(c)  $\Delta m_{atm}^2$  vs  $m_{lightest}$  for  $\varphi_1 = 200^\circ$



(d)  $\Delta m_{sol}^2$  vs  $m_{lightest}$  for  $\varphi_1 = 200^\circ$



(e)  $\Delta m_{atm}^2$  vs  $m_{lightest}$  for  $\varphi_1 = 300^\circ$



(f)  $\Delta m_{sol}^2$  vs  $m_{lightest}$  for  $\varphi_1 = 300^\circ$

Figure 3.6: This is  $\Delta m_{atm}^2$  vs  $m_{lightest}$  and  $\Delta m_{sol}^2$  vs  $m_{lightest}$  trend with fixed  $\varphi_1$  and varying  $\varphi_2$ . Fixed values of neutrino mixing angles are mentioned at the top.  $\varphi_1 = 100^\circ$  and different  $\varphi_2$  values within a graph are denoted by different colours as indicated by the legends. Solid lines represent that all neutrino angles for that pair of Majorana phases are inside their corresponding 3- $\sigma$  ranges and dotted lines represent that all angles are NOT inside the 3- $\sigma$  ranges. Curved lines correspond to  $\Delta m_{atm}^2$  or  $\Delta m_{sol}^2$  and the straight lines correspond to  $m_{\beta\beta}$ .

take values much lesser than what is required of them to be in the valid range. But comparing it to the Fig.(3.6d), we understand that there is a finite overlap of  $m_{lightest}$  values for which both  $\Delta m_{atm}^2$  and  $m_{\beta\beta}$  lie within their valid  $3-\sigma$  ranges. In conclusion, we can say that for  $\varphi_1 = 200^\circ$ , we can find three  $\varphi_2$  values for which we can have three neutrino angles and  $\Delta m_{sol}^2$  that can be brought inside without dismissing the  $m_{\beta\beta}$  constraint.

The discussion for Fig.(3.6e) and Fig.(3.6f) is pretty much the same, except for the fact that there is only one solid line present. This means, that only one pair of  $\varphi_1$  and  $\varphi_2$ , out of the chosen ones, brings all angles inside. Furthermore, just like in the previous case,  $\Delta m_{atm}^2$  has low values below the  $m_{\beta\beta}$  upper bound and it's only  $\Delta m_{sol}^2$  which is inside its range for  $m_{lightest}$  values corresponding to valid  $m_{\beta\beta}$  values. If this case holds true, then the mass value of the lightest neutrino is roughly around  $0.15eV$  at the present scale (MZ scale), which is very low.

### 3.5 Conclusion from HSMU hypothesis

HSMU successfully verifies the radiative magnification of neutrino mixing angles, as suggested by the corresponding RG equations [Eq.(2.1), (2.2) and (2.3)]. It also suggests normal ordering (N.O.) for neutrino masses, as the radiative magnification isn't achieved by inverted ordering (I.O.). It also verifies quasi-degeneracy of neutrino masses as shown in Fig.(3.1b).

HSMU completely discards the possibility of neutrinos being Dirac particles [section(3.3.1)], as neither in CP conserving nor in CP violating case neutrino angles satisfy their  $3 - \sigma$  bounds.

HSMU fails to bring in all five parameters also in Majorana case[refer section(3.3.2)] where Majorana phases are taken to be zero. In the case, when Majorana phases are non-zero, it can bring at the most four out of five low scale parameters inside  $3 - \sigma$  ranges. The additional experimental upper bound of  $m_{\beta\beta}$  is respected in a few cases. But in no case, all six(three angles, two mass squared differences and  $m_{\beta\beta}$ ) could satisfy their valid bounds simultaneously.



# Chapter 4

## Wolfenstein Parameterization

### 4.1 Background

It was evident from previous chapter that without corrections to  $\Delta m_{sol}^2$  or  $\Delta m_{atm}^2$ , in no case, HSMU brings all low scale neutrino parameters inside their 3- $\sigma$  ranges. For this reason, we will like to consider another ansatz which tries to explain the hierarchical nature of neutrino mixing angles. This ansatz lifts the stricter restrictions on high scale neutrino mixing angles put by HSMU. In HSMU we consider that neutrino mixing angles are exactly equal to those of quarks at high scale (GUT scale). But now instead of exact values, we consider that the hierarchy in high scale quark mixing angle is duplicated in neutrinos' angles. This hierarchy is parameterized by a particular method called *Wolfenstein Parameterization*.

In Wolfenstein parameterization we consider neutrino mixing angles to be like following-

$$\begin{aligned}\sin \theta_{12} &= \lambda \\ \sin \theta_{23} &= \lambda^2 \\ \sin \theta_{23} &= \lambda^3\end{aligned}\tag{4.1}$$

where  $\lambda$  is called Wolfenstein parameter which is also the sine of solar mixing angle. Note that this is not to be confused with Higgs' quartic coupling. Wolfenstein parameter gives the neutrino mixing angles the following hierarchical structure-

$$\begin{aligned}\theta_{12} &= \arcsin(\lambda) \\ \theta_{23} &= \arcsin(\lambda^2) \\ \theta_{13} &= \arcsin(\lambda^3)\end{aligned}\tag{4.2}$$

We can vary  $\theta_{23}$  and  $\theta_{13}$  more finely by introducing  $\alpha$  and  $\beta$  such that  $\alpha, \beta > 0$ , Eq.(4.2) can be modified into -

$$\begin{aligned}\theta_{12} &= \arcsin(\lambda) \\ \theta_{23} &= \alpha \arcsin(\lambda^2) \\ \theta_{13} &= \beta \arcsin(\lambda^3)\end{aligned}\tag{4.3}$$

Note that, choosing  $\lambda$  to be equal to 0.22532,  $\alpha$  to be equal to 0.698353 and  $\beta$  to be equal to 0.264066 we get back the HSMU ansatz. For the initial study of Wolfenstein ansatz, we analyze the effects of varying  $\alpha$  and  $\beta$  keeping Majorana phases to be zero and  $\lambda$  equal to a value corresponding to HSMU ansatz( $\lambda_{HSMU} = 0.22532$ ). Once we find a suitable pair of  $\alpha, \beta$ , we can study variations in  $\lambda$ . Only after thoroughly analyzing effects of  $\alpha, \beta$  and  $\lambda$  we will bring in non-zero Majorana phases into the picture. CP violation phase is taken to be equal to that of quarks' CP violation phase( $\delta_q$ ) in all the cases.

## 4.2 Results and discussions

### 4.2.1 Variations of $\alpha$ and $\beta$

The reason we must first study variations of  $\alpha$  and  $\beta$  is that- changing them can change the hierarchy of the angles at high scale which can possibly alter the usual RG running of the angles. Hence, to study variations of  $\alpha, \beta$  we observe how the angles evolve for each pair of  $\alpha, \beta$  we choose.

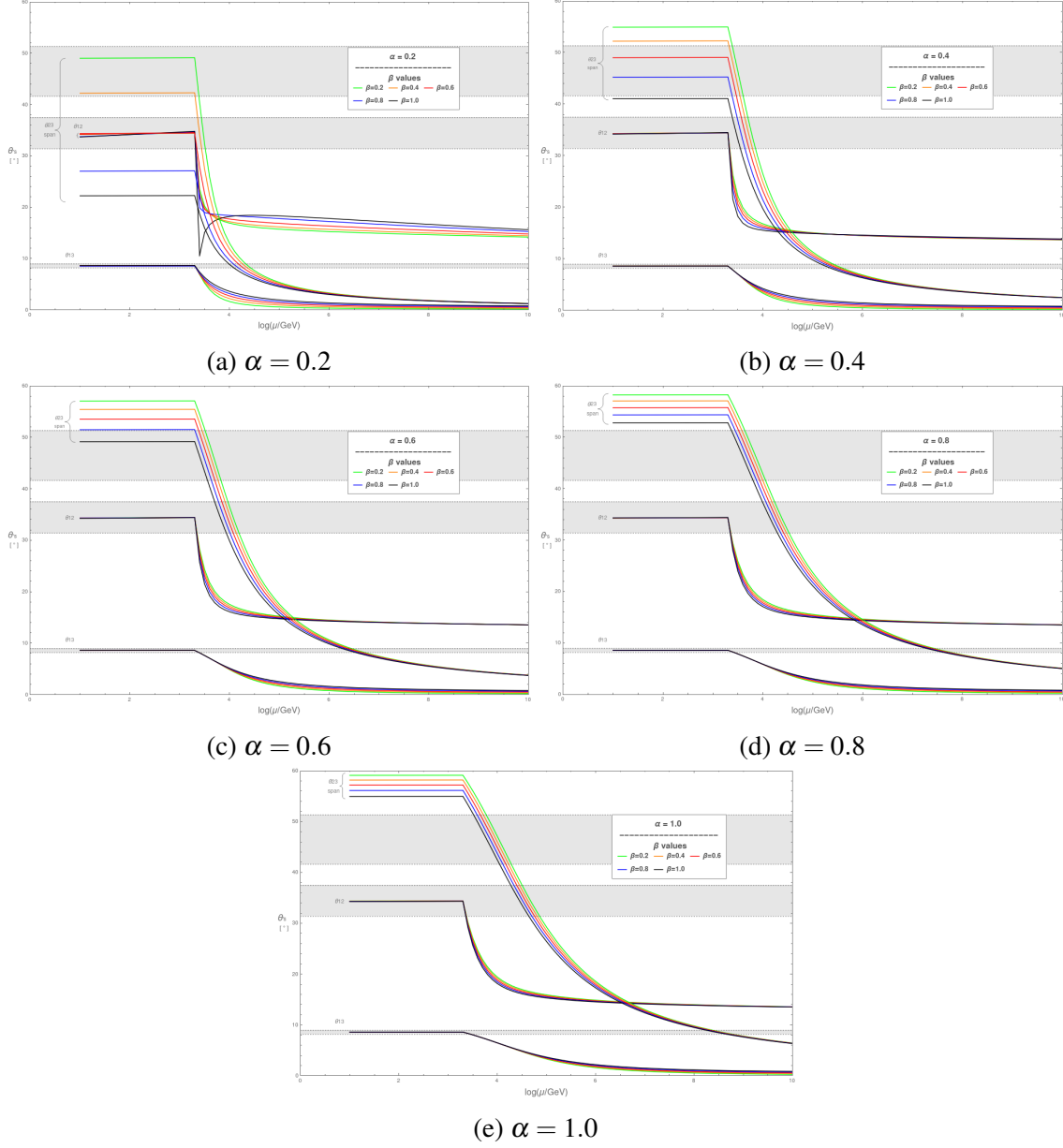


Figure 4.1: This is RG running of neutrino mixing angles for various  $\alpha$ ,  $\beta$  pairs. Value of  $\alpha$  is kept fixed and  $\beta$  is varied, represented by different colours. The shaded regions show  $3 - \sigma$  ranges for all three angles. For all the graphs  $\lambda = \lambda_{HSMU} = 0.22532$ .

To obtain the graphs in Fig.(4.1) Neutrino masses at high scales are chosen such that  $\theta_{12}$  and  $\theta_{13}$  are at their best fit value at low scale and  $\theta_{23}$  at low scale is allowed to vary. The trend across the graphs shows that as  $\alpha$  increases the span of  $\theta_{23}$  shrinks and shifts higher in values. As a result of this, for a particular value of  $\alpha$ , only for a few number of  $\beta$  values, all three angles have values

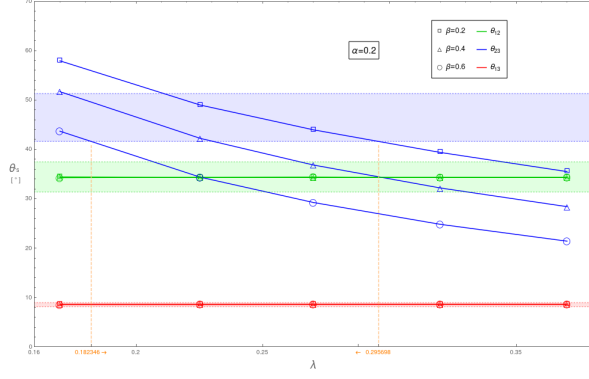
within their experimental  $3 - \sigma$  range. From Fig.(4.1d) and Fig.(4.1e) it can be seen that the entire span of  $\theta_{23}$  lies outside of its valid range, i.e. for  $\alpha = 0.8$  and  $\alpha = 1.0$ , we can not have all three mixing angles inside their valid ranges.

Having discussed about value of  $\theta_{23}$  at low scale, let's now focus on the RG running pattern. All the runnings for all the graphs look quite normal, except for one case. For  $\alpha = 0.2$  and  $\beta = 1.0$  [Fig.(4.1a)], the RG flow of  $\theta_{12}$  is non-differentiable at one more point other than at SUSY breaking scale. That is, the graph shows a kink just after SUSY breaking scale. Since we are varying  $\beta$  discretely, one must take into account that this feature is arising when  $\beta$  transitions from values 0.8 to 1.0. Because of this unusual RG running values of neutrino masses at low scale will also get affected and hence we will ignore the pairs  $\alpha = 0.2, \beta = 0.8$  and  $\alpha = 0.2, \beta = 1.0$  for  $\lambda$  variations. We continue with the remaining pairs of  $\alpha, \beta$  and check how low scale parameters behave when we now additionally vary  $\lambda$  too.

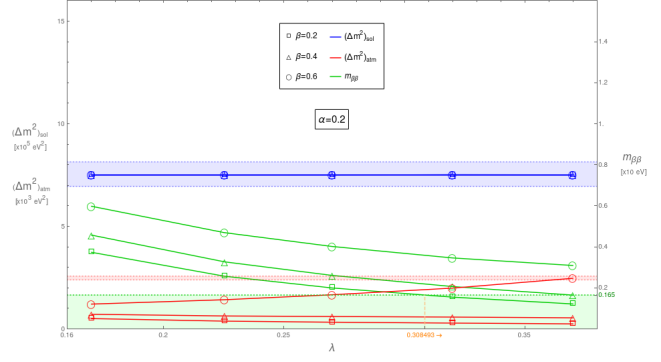
## 4.2.2 Variation of $\lambda$

Out of 25 pairs of  $\alpha, \beta$  we chose 23 valid pairs for which we analyze low scale values of  $\theta_{12}, \theta_{23}, \theta_{13}, \Delta m_{sol}^2, \Delta m_{atm}^2$  as well as  $m_{\beta\beta}$ . Note that we still will have Majorana phases to be zero. Its effects are to be seen later. Fig(4.2) shows all low scale parameter vs  $\lambda$ .

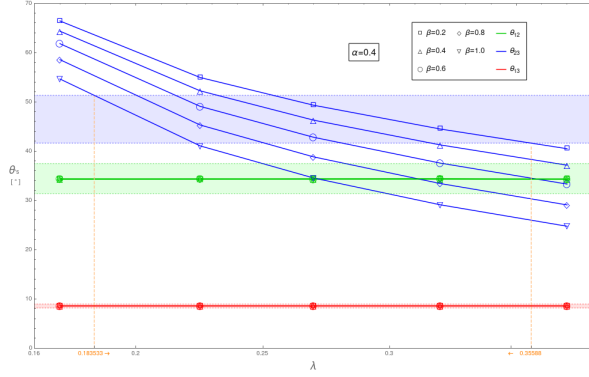
We use three degrees of freedom (high scale masses) to fix  $\theta_{12}, \theta_{13}$  and  $\Delta m_{sol}^2$  at their best fit values. Thus  $\theta_{23}, \Delta m_{atm}^2$  and  $m_{\beta\beta}$  are set free. As we can see  $\theta_{23}$  and  $m_{\beta\beta}$  values decrease for increasing  $\lambda$ . While doing so, they cross their valid range. The minimum value of  $\lambda$  for which this happens, is highlighted on X-axis. For a specific pair of  $\alpha$  and  $\beta$  we can compare these minimum values of  $\lambda$  above which all angles and  $m_{\beta\beta}$  can be brought inside their respective  $3 - \sigma$  ranges. In  $\alpha = 0.2$  case[Fig.(4.2a) and Fig.(4.2b)], the  $\lambda$  -space for which all angles are inside valid ranges does NOT overlap with  $\lambda$  -space for which  $m_{\beta\beta}$  is inside its  $3 - \sigma$  range. Thus, for  $\alpha = 0.2$  we can, at the best, bring 4 out of 6 parameters inside. But still this scenario is a little better than that in HSMU case, where we could not even bring all three angles inside their range. This is an indication that



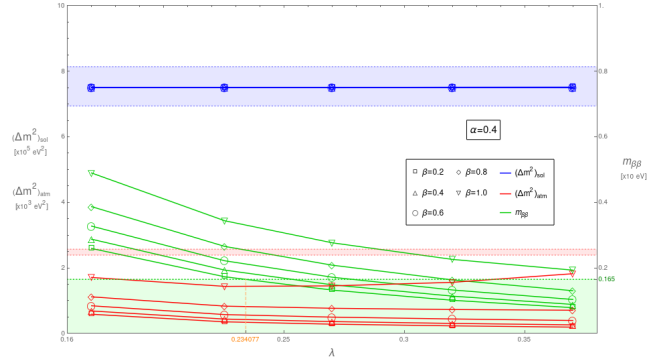
(a)  $\theta_{12}, \theta_{23}, \theta_{13}$  vs  $\lambda$  for  $\alpha = 0.2$



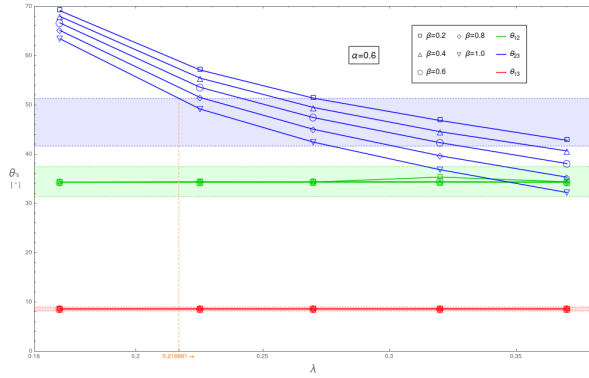
(b)  $\Delta m_{sol}^2, \Delta m_{atm}^2, m_{\beta\beta}$  vs  $\lambda$  for  $\alpha = 0.2$



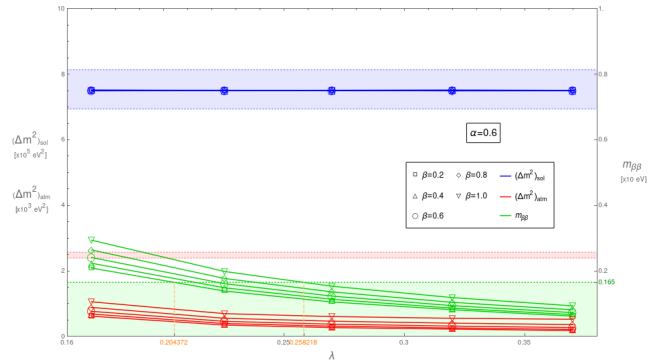
(c)  $\theta_{12}, \theta_{23}, \theta_{13}$  vs  $\lambda$  for  $\alpha = 0.4$



(d)  $\Delta m_{sol}^2, \Delta m_{atm}^2, m_{\beta\beta}$  vs  $\lambda$  for  $\alpha = 0.4$

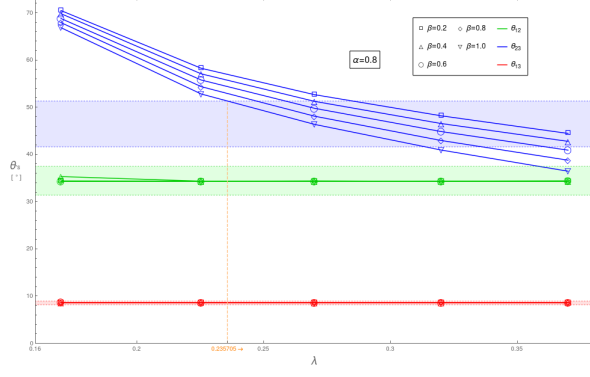


(e)  $\theta_{12}, \theta_{23}, \theta_{13}$  vs  $\lambda$  for  $\alpha = 0.6$

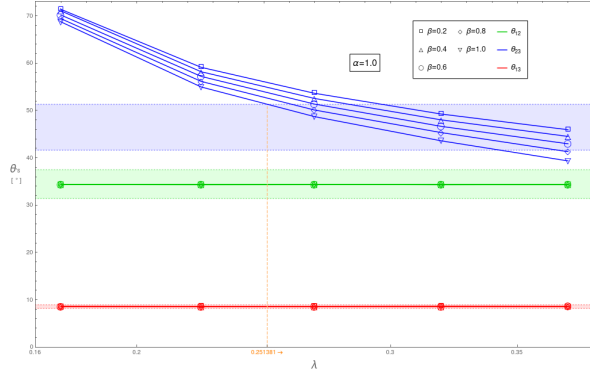


(f)  $\Delta m_{sol}^2, \Delta m_{atm}^2, m_{\beta\beta}$  vs  $\lambda$  for  $\alpha = 0.6$

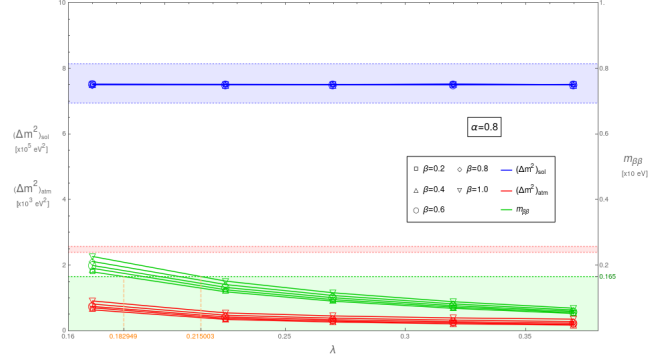
Wolfenstein parameterization is improving the results. For next set of  $\alpha$  values, it gets even better. We can find an overlap between  $\lambda$  -spaces of angles' graph and  $m_{\beta\beta}$  's graph for same  $\alpha$ . It means that for those  $\lambda$  values, we can bring in all angles,  $\Delta m_{sol}^2$  as well as  $m_{\beta\beta}$  inside their 3 -  $\sigma$  ranges, i.e. 5 out of 6 parameters. Further, we will switch on the Majorana phases ( $\varphi_1, \varphi_2$ ) and study its effects on all 6 low scale parameters. The aim is to bring in all 6 parameters inside.



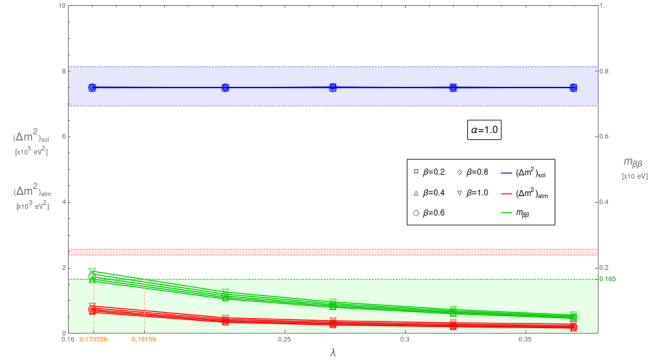
(g)  $\theta_{12}, \theta_{23}, \theta_{13}$  vs  $\lambda$  for  $\alpha = 0.8$



(i)  $\theta_{12}, \theta_{23}, \theta_{13}$  vs  $\lambda$  for  $\alpha = 1.0$



(h)  $\Delta m_{sol}^2, \Delta m_{atm}^2, m_{\beta\beta}$  vs  $\lambda$  for  $\alpha = 0.8$



(j)  $\Delta m_{sol}^2, \Delta m_{atm}^2, m_{\beta\beta}$  vs  $\lambda$  for  $\alpha = 1.0$

Figure 4.2: This is variation in various low scale parameter values (represented by different colours) against  $\lambda$ . For a single graph, value of  $\alpha$  is kept fixed and  $\beta$  is varied, represented by different shapes on the curves. The shaded regions show  $3 - \sigma$  ranges for all three angles, mass square differences and  $m_{\beta\beta}$ .

### 4.2.3 $\varphi_1, \varphi_2$ variations

With these independent parameters we will not span the entire  $\varphi_1, \varphi_2$  space unnecessarily, as the final goal is to find any set of input parameters for which all 6 parameters (angles, mass squared differences,  $m_{\beta\beta}$ ) are inside their  $3 - \sigma$  ranges at low scale and thereby, strengthening the possibility of Wolfenstein ansatz.

We focus on the parameters which are set free to vary, i.e.,  $\theta_{23}$ ,  $\Delta m_{atm}^2$  and  $m_{\beta\beta}$ . This is because other parameters are held constant at their best fit values using three independent parameters- high scale neutrino masses. Thus, the newly introduced parameters  $\lambda$ ,  $\alpha$  and  $\beta$  along with Majorana phases can be used to manipulate low scale values of  $\theta_{23}$ ,  $\Delta m_{atm}^2$  and  $m_{\beta\beta}$ .

To have a simple and convenient start, we use the HSMU case to pick up only those  $\varphi_1, \varphi_2$  pairs for which we could bring in all angles and one of the mass squared differences inside valid ranges. From the Table.(3.3), we choose these values of  $\varphi_1, \varphi_2$  -

- $\varphi_1 = 50^\circ ; \varphi_2 = 0^\circ$
- $\varphi_1 = 50^\circ ; \varphi_2 = 300^\circ$
- $\varphi_1 = 200^\circ ; \varphi_2 = 300^\circ$
- $\varphi_1 = 300^\circ ; \varphi_2 = 50^\circ$

**The plan:** For these values, we shall discretely vary  $\alpha$  and  $\beta$ . From  $\alpha, \beta$  and  $\lambda$  variations [Fig.(4.2)], it is observed that as  $\lambda$  increases,  $\theta_{23}, \Delta m_{atm}^2$  and  $m_{\beta\beta}$  decrease and vice versa. An exception to this trend is observed at lower values of  $\alpha$ , where  $\Delta m_{atm}^2$  behaves the opposite for larger values of  $\lambda$ . One more reason to ignore low  $\alpha$  values is that the span of  $\theta_{23}$  is larger than its  $3 - \sigma$  range. Because of this, all  $\beta$  values for, say  $\alpha = 0.2$  and  $\alpha = 0.4$ , can not bring  $\theta_{23}$  value inside its  $3 - \sigma$  range. This makes them less probable candidates for  $\lambda$  variations.

Keeping this in mind, we ignore the lower  $\alpha$  values and check  $\lambda$  variations for them in future. For now, we shall only vary  $\lambda$  for those pairs of  $\varphi_1, \varphi_2$  for which  $\theta_{23}, \Delta m_{atm}^2$  and  $m_{\beta\beta}$  are all either above/below their  $3 - \sigma$  ranges simultaneously or are all inside their  $3 - \sigma$  ranges simultaneously. This is because if one of the parameters from  $\theta_{23}, \Delta m_{atm}^2$  and  $m_{\beta\beta}$  lies on one side (higher or lower) of its own  $3 - \sigma$  range and other parameter lies on the opposite side of its own  $3 - \sigma$  range, changing  $\lambda$  will result in shifting one of the parameters away from its  $3 - \sigma$  range and thus not letting us bring in all 6 low scale parameters in their valid experimental bounds. This plan is case-wise realised in the following sub-section.

#### 4.2.4 $\alpha, \beta, \lambda, \varphi_1, \varphi_2$ variations combined

Now we shall choose the aforementioned  $\varphi_1, \varphi_2$  pairs for  $\alpha, \beta$  variation and select only those values for  $\lambda$  variations, for which  $\theta_{23}, \Delta m_{atm}^2$  and  $m_{\beta\beta}$  lie on one side of their respective  $3 - \sigma$  range. To illustrate this, a symbolic notation is used in order to understand the increasing/decreasing trend

of these parameters.

Using various colours and shapes, Tables(4.1 and 4.2) illustrate whether the respective parameter is inside, above or below the respective  $3 - \sigma$  ranges for various pairs of  $\alpha$ ,  $\beta$  and  $\varphi_1$ ,  $\varphi_2$ . As discussed above, we ignore the lower values of  $\alpha$  (0.4 and 0.2) as the  $\lambda$  variations don't assure either monotonic increase or monotonic decrease in  $\Delta m_{atm}^2$ , for these  $\alpha$  values. So in the rest, we want to get rid of those  $\alpha$ ,  $\beta$  pairs for which any two low scale parameters lie on opposite sides of their respective  $3 - \sigma$  ranges. In the symbolic representation, this translates to ruling out those data sets which have both green and red coloured symbols for the same  $\alpha$ ,  $\beta$  pairs. Let's consider the four cases one by one.

**Case-1:**  $\varphi_1 = 50^\circ$  and  $\varphi_2 = 0^\circ$

From the case when  $\varphi_1$ ,  $\varphi_2$  are  $50^\circ$  and  $0^\circ$  respectively [Table(4.1a)], we can see that red and green symbols occur together for every  $\alpha$ ,  $\beta$  pairs. Thus we can choose to ignore them for  $\lambda$  variations as it signifies that there exists at least one parameter among  $\theta_{23}$ ,  $\Delta m_{atm}^2$  and  $m_{\beta\beta}$ , which does NOT come inside its valid  $3 - \sigma$  range. Since this happens for every  $\alpha$ ,  $\beta$  pair, it leaves us with no plausible sets of  $\alpha$ ,  $\beta$  pairs for  $\lambda$  variations. Thus we can arguably rule out the Majorana phases pair ( $50^\circ, 300^\circ$ ) as a candidate to bring in all six low scale parameters.

**Case-2:**  $\varphi_1 = 50^\circ$  and  $\varphi_2 = 300^\circ$

From the case when  $\varphi_1$ ,  $\varphi_2$  are  $50^\circ$  and  $300^\circ$  respectively [Table(4.1b)], we can see that every time red and green symbols occur together for the same  $\alpha$ ,  $\beta$  pairs we can choose to ignore them for  $\lambda$  variations as it signifies that there exists at least one parameter among  $\theta_{23}$ ,  $\Delta m_{atm}^2$  and  $m_{\beta\beta}$ , which does NOT come inside its valid  $3 - \sigma$  range. This leaves us with only five plausible sets of  $\alpha$ ,  $\beta$  pairs. They are as follows-

- $\alpha = 1.0$  ;  $\beta = 0.8$
- $\alpha = 1.0$  ;  $\beta = 0.6$
- $\alpha = 0.8$  ;  $\beta = 1.0$
- $\alpha = 0.8$  ;  $\beta = 0.4$
- $\alpha = 0.6$  ;  $\beta = 0.2$

$\alpha$	$\beta$	$\theta_{23}$	$\Delta m_{atm}^2$	$m_{\beta\beta}$
1.0	1.0	●	●	●
1.0	0.8	*	●	*
1.0	0.6	*	●	●
1.0	0.4	●	●	●
1.0	0.2	●	●	●
0.8	1.0	*	●	●
0.8	0.8	●	●	●
0.8	0.6	*	●	●
0.8	0.4	*	●	●
0.8	0.2	●	●	●
0.6	1.0	●	●	●
0.6	0.8	*	●	●
0.6	0.6	●	●	●
0.6	0.4	*	●	●
0.6	0.2	*	●	●
0.4	1.0	●	●	●
0.4	0.8	●	●	●
0.4	0.6	●	●	●
0.4	0.4	*	●	●
0.4	0.2	*	●	●
0.2	1.0	●	●	●
0.2	0.8	●	●	●
0.2	0.6	●	●	●
0.2	0.4	●	●	●
0.2	0.2	*	●	●

(a) For  $\varphi_1 = 50^\circ$  and  $\varphi_2 = 0^\circ$

$\alpha$	$\beta$	$\theta_{23}$	$\Delta m_{atm}^2$	$m_{\beta\beta}$
1.0	1.0	●	●	●
1.0	0.8	*	●	●
1.0	0.6	*	●	●
1.0	0.4	*	●	●
1.0	0.2	*	●	●
0.8	1.0	*	●	●
0.8	0.8	●	●	●
0.8	0.6	●	●	*
0.8	0.4	*	●	●
0.8	0.2	*	●	●
0.6	1.0	●	●	●
0.6	0.8	*	●	●
0.6	0.6	●	●	●
0.6	0.4	●	●	*
0.6	0.2	*	●	*
0.4	1.0	●	●	●
0.4	0.8	●	●	●
0.4	0.6	●	●	●
0.4	0.4	●	●	●
0.4	0.2	●	●	●
0.2	1.0	●	●	●
0.2	0.8	●	●	●
0.2	0.6	●	●	●
0.2	0.4	●	●	●
0.2	0.2	*	●	●

(b) For  $\varphi_1 = 50^\circ$  and  $\varphi_2 = 300^\circ$

Table 4.1: Qualitative trends of  $\theta_{23}$ ,  $\Delta m_{atm}^2$  and  $m_{\beta\beta}$  with  $\alpha$  and  $\beta$  for  $\lambda = \lambda_{HSMU}$ . The coloured symbols represent the following-

- : Parameter value is inside  $3 - \sigma$  range
- : Parameter value is below its lower bound
- : Parameter value is above its upper bound
- \*: Parameter value is inside, but near the  $3 - \sigma$  boundary
- \*: Parameter value is *just* below its lower bound
- \*: Parameter value is *just* above its lower bound

In all these pairs, except for  $\alpha = 0.8, \beta = 1.0$ ,  $\Delta m_{atm}^2$  is below its lower bound and in order to correct it we will have to decrease  $\lambda$  such that  $\Delta m_{atm}^2$  increases. But note that for all these pairs

of  $\alpha$  and  $\beta$ ,  $\theta_{23}$  is given by ‘ $\star$ ’, representing that  $\theta_{23}$  is on the edge of its  $3 - \sigma$  range. The appendix[A.1b] shows that its near its *upper bound* and not the lower one. Thus decreasing  $\lambda$  would shift  $\theta_{23}$  immediately out of its valid range and we won’t be able to get  $\theta_{23}$  inside when  $\Delta m_{atm}^2$  comes inside  $3 - \sigma$  range. In the case when  $\alpha = 0.8$  and  $\beta = 1.0$ , the opposite argument applies.  $\lambda$  has to be increased in order to bring  $\Delta m_{atm}^2$  inside  $3 - \sigma$  range. But while doing so,  $\theta_{23}$ , which is now near its lower bound will decrease and move out of its  $3 - \sigma$  range. This makes it impossible again to bring all six low scale parameters in. Thus we can again arguably rule out the Majorana phases pair  $(50^\circ, 300^\circ)$  as a candidate to bring in all six low scale parameters.

**Case-3:**  $\varphi_1 = 200^\circ$  and  $\varphi_2 = 300^\circ$

From the case when  $\varphi_1, \varphi_2$  are  $200^\circ$  and  $300^\circ$  respectively [Table(4.2a)], we again choose to ignore simultaneous occurrences of red and green together for  $\lambda$  variations. This leaves us with only three plausible sets of  $\alpha, \beta$  pairs. They are as follows-

- $\alpha = 1.0 ; \beta = 0.4$
- $\alpha = 1.0 ; \beta = 0.2$
- $\alpha = 0.8 ; \beta = 0.4$

In all these pairs,  $\Delta m_{atm}^2$  is below its lower bound and in order to correct it, we will have to decrease  $\lambda$  such that  $\Delta m_{atm}^2$  increases. But note that for two of these pairs of  $\alpha$  and  $\beta$ ,  $\theta_{23}$  is given by ‘ $\star$ ’, representing that  $\theta_{23}$  is on the edge of its  $3 - \sigma$  range. The appendix[A.2a] shows that its near its *upper bound* and not the lower one. Thus decreasing  $\lambda$  would shift  $\theta_{23}$  immediately out of its valid range and we won’t be able to get  $\theta_{23}$  inside when  $\Delta m_{atm}^2$  comes inside  $3 - \sigma$  range. Upon decreasing  $\lambda$  for the remaining case when  $\alpha = 1.0$  and  $\beta = 0.2$ , the same argument applies even though  $\theta_{23}$  value is inside  $3 - \sigma$  range. That is, it shifts  $\theta_{23}$  again out of its valid range and  $\Delta m_{atm}^2$  still doesn’t come inside. This makes it impossible again to bring all six low scale parameters in. Thus we can again arguably rule out the Majorana phases pair  $(200^\circ, 300^\circ)$  as a candidate to bring in all six low scale parameters.

$\alpha$	$\beta$	$\theta_{23}$	$\Delta m_{atm}^2$	$m_{\beta\beta}$
1.0	1.0	●	●	●
1.0	0.8	★	●	●
1.0	0.6	★	●	●
1.0	0.4	★	●	●
1.0	0.2	●	●	●
0.8	1.0	●	●	●
0.8	0.8	●	●	●
0.8	0.6	★	●	●
0.8	0.4	★	●	●
0.8	0.2	●	●	★
0.6	1.0	●	●	●
0.6	0.8	●	●	●
0.6	0.6	●	●	●
0.6	0.4	★	●	●
0.6	0.2	●	●	●
0.4	1.0	●	●	●
0.4	0.8	●	●	●
0.4	0.6	●	●	●
0.4	0.4	★	●	●
0.4	0.2	★	●	●
0.2	1.0	●	●	●
0.2	0.8	●	●	●
0.2	0.6	●	●	●
0.2	0.4	●	●	●
0.2	0.2	★	●	●

(a) For  $\varphi_1 = 200^\circ$  and  $\varphi_2 = 300^\circ$

$\alpha$	$\beta$	$\theta_{23}$	$\Delta m_{atm}^2$	$m_{\beta\beta}$
1.0	1.0	★	●	●
1.0	0.8	★	●	●
1.0	0.6	★	●	●
1.0	0.4	★	●	●
1.0	0.2	★	●	●
0.8	1.0	★	●	●
0.8	0.8	★	●	●
0.8	0.6	★	●	●
0.8	0.4	★	●	●
0.8	0.2	★	●	●
0.6	1.0	★	●	●
0.6	0.8	★	●	●
0.6	0.6	★	●	●
0.6	0.4	★	●	●
0.6	0.2	★	●	●
0.4	1.0	★	●	●
0.4	0.8	★	●	●
0.4	0.6	★	●	●
0.4	0.4	★	●	●
0.4	0.2	★	●	●
0.2	1.0	★	●	★
0.2	0.8	★	●	●
0.2	0.6	★	●	●
0.2	0.4	★	●	●
0.2	0.2	★	●	●

(b) For  $\varphi_1 = 300^\circ$  and  $\varphi_2 = 50^\circ$

Table 4.2: Qualitative trends of  $\theta_{23}$ ,  $\Delta m_{atm}^2$  and  $m_{\beta\beta}$  with  $\alpha$  and  $\beta$  for  $\lambda = \lambda_{HSMU}$ . The coloured symbols represent the following-

- : Parameter value is inside  $3 - \sigma$  range
- : Parameter value is below its lower bound
- : Parameter value is above its upper bound
- ★: Parameter value is inside, but near the  $3 - \sigma$  boundary
- ★: Parameter value is *just* below its lower bound
- ★: Parameter value is *just* above its lower bound

**Case-4:**  $\varphi_1 = 300^\circ$  and  $\varphi_2 = 50^\circ$

From the case when  $\varphi_1, \varphi_2$  are  $300^\circ$  and  $50^\circ$  respectively [Table(4.2b)], we again choose to ignore simultaneous occurrences of red and green together for  $\lambda$  variations. This time it leaves us with

some better results. It gives us total 13 plausible sets of  $\alpha$ ,  $\beta$  pairs for which we can hope to look for  $\lambda$  variations. They are as follows-

- $\alpha = 1.0 ; \beta = 1.0$
- $\alpha = 0.8 ; \beta = 1.0$
- $\alpha = 0.8 ; \beta = 0.8$
- $\alpha = 0.6 ; \beta = 1.0$
- $\alpha = 0.6 ; \beta = 0.8$
- $\alpha = 0.6 ; \beta = 0.6$
- $\alpha = 0.6 ; \beta = 0.4$
- $\alpha = 0.4 ; \beta = 1.0$
- $\alpha = 0.4 ; \beta = 0.8$
- $\alpha = 0.4 ; \beta = 0.6$
- $\alpha = 0.4 ; \beta = 0.4$
- $\alpha = 0.4 ; \beta = 0.2$
- $\alpha = 0.2 ; \beta = 1.0$

In all these pairs,  $\Delta m_{atm}^2$  is again below its lower bound. But notice that the plausible sets now have majority of values for which  $\alpha$  's are lower in value. Recall that we decided to ignore lower values of  $\alpha$  because in vanishing  $\varphi_1$ ,  $\varphi_2$  case,  $\Delta m_{atm}^2$  doesn't show monotonic increase or monotonic decrease for some values of  $\beta$ . Thus for lower values of  $\alpha$ , unless calculated we can't speculate the trend of  $\Delta m_{atm}^2$  with  $\lambda$ . In order to correct  $\Delta m_{atm}^2$ , we may have to decrease *or* increase  $\lambda$ . But note that for all of these pairs of  $\alpha$  and  $\beta$ ,  $\theta_{23}$  is given by ' $\star$ ', representing that  $\theta_{23}$  is on the edge of its  $3 - \sigma$  range. The appendix[A.2b] shows that its near its *upper bound* and not the lower one. Thus decreasing  $\lambda$  would shift  $\theta_{23}$  immediately out of its valid range and we won't be able to get  $\theta_{23}$  inside when  $\Delta m_{atm}^2$  comes inside  $3 - \sigma$  range. Thus increasing  $\lambda$  seems to be only option in order to create a possibility to bring in all six parameters. Note again that this variation does NOT assure getting the desired results. Only in the possibility where  $\Delta m_{atm}^2$  increases with increasing  $\lambda$ , we might approach our desired goal. In case of failure of this case as well, we would have to thoroughly judge the other  $\varphi_1$ ,  $\varphi_2$  pairs apart from these four.

# Chapter 5

## Summary and outlook

In conclusion, HSMU hypothesis discards the case when neutrinos are considered Dirac particles as all mixing angles at low scale do not lie in their corresponding  $3\text{-}\sigma$  range values. When neutrinos are considered as Majorana particles, one can find non-zero Majorana phase values for which low scale values of all mixing angles and one of the mass squared differences along with  $m_{\beta\beta}$  value can be brought inside their valid ranges. But since all low scale parameter values can still not be brought in the  $3\text{-}\sigma$  range, HSMU doesn't hold true in this case too. Thus HSMU in the standard parameterization, fails to explain non-zero neutrino mixing angles.

HSMU in Wolfenstein parameterization shows some hope for positive results. Involving more degrees of freedom in the theory helps us manage to get most of the low scale values along with  $m_{\beta\beta}$  inside their respective  $3\text{-}\sigma$  ranges. Thus Wolfenstein ansatz is proven to be a better candidate model to explain neutrino mixing angles' values and hierarchy.

**Outlook:** Wolfenstein ansatz may accommodate a set of independent parameters for which ALL low scale parameters could be brought inside their valid ranges. Therefore further analysis of Wolfenstein ansatz is required in order to find a full space of independent parameters. In case, the situation doesn't improve, threshold corrections might be needed. Moreover, various other variations like  $\delta_{CP}$ , SUSY scale, *GUT* scale variation can be analysed for the same.



# Bibliography

- [1] Ivan Esteban, M. C. Gonzalez-Garcia, Michele Maltoni, Thomas Schwetz, and Albert Zhou. The fate of hints: updated global analysis of three-flavor neutrino oscillations. *JHEP*, 09:178, 2020.
- [2] H. Baer and X. Tata. *Weak scale supersymmetry: From superfields to scattering events*. Cambridge University Press, 5 2006.
- [3] A. Broncano, M. B. Gavela, and Elizabeth Ellen Jenkins. The Effective Lagrangian for the seesaw model of neutrino mass and leptogenesis. *Phys. Lett. B*, 552:177–184, 2003. [Erratum: *Phys.Lett.B* 636, 332 (2006)].
- [4] Stefan Antusch, Jörn Kersten, Manfred Lindner, and Michael Ratz. Running neutrino masses, mixings and CP phases: Analytical results and phenomenological consequences. *Nucl. Phys. B*, 674:401–433, 2003.
- [5] P. M. Watkins. DISCOVERY OF THE W AND Z BOSONS. *Contemp. Phys.*, 27:291–324, 1986.
- [6] P. L. Tipton and T. M. Liss. The Discovery of the Top Quark. *Scientific American*, 277 (3):54–59, 1997.
- [7] J. E. Augustin et al. Discovery of a Narrow Resonance in  $e^+e^-$  Annihilation. *Phys. Rev. Lett.*, 33:1406–1408, 1974.
- [8] J. J. Aubert et al. Experimental Observation of a Heavy Particle *J. Phys. Rev. Lett.*, 33:1404–1406, 1974.
- [9] John N. Bahcall and Raymond Davis. Solar neutrinos: A scientific puzzle. *Science*, 191(4224):264–267, 1976.
- [10] Q. R. Ahmad and Others. Measurement of the rate of  $\nu_e + d \rightarrow p + p + e^-$  interactions produced by  $^8\text{B}$  solar neutrinos at the sudbury neutrino observatory. *Phys. Rev. Lett.*, 87:071301, Jul 2001.
- [11] Y. Fukuda et al. Evidence for oscillation of atmospheric neutrinos. *Phys. Rev. Lett.*, 81:1562–1567, 1998.

- [12] L. A. Mikaelyan and V. V. Sinev. Neutrino oscillations at reactors: What next? *Phys. Atom. Nucl.*, 63:1002–1006, 2000.
- [13] Q. R. Ahmad et al. Direct evidence for neutrino flavor transformation from neutral current interactions in the Sudbury Neutrino Observatory. *Phys. Rev. Lett.*, 89:011301, 2002.
- [14] Y. Fukuda et al. Measurement of the flux and zenith angle distribution of upward through going muons by Super-Kamiokande. *Phys. Rev. Lett.*, 82:2644–2648, 1999.
- [15] K. Eguchi et al. First results from KamLAND: Evidence for reactor anti-neutrino disappearance. *Phys. Rev. Lett.*, 90:021802, 2003.
- [16] Particle Data Group. Review of Particle Physics. *Progress of Theoretical and Experimental Physics*, 2020(8), 08 2020. 083C01.
- [17] R. N. Mohapatra, M. K. Parida, and G. Rajasekaran. High scale mixing unification and large neutrino mixing angles. *Phys. Rev. D*, 69:053007, 2004.
- [18] I. Antoniadis, E. Dudas, D. M. Ghilencea, and P. Tziveloglou. MSSM with dimension-five operators (MSSM5). *Nuclear Physics B*, 808(1):155–184, 2009.
- [19] P. F. de Salas, D. V. Forero, S. Gariazzo, P. Martínez-Miravé, O. Mena, C. A. Ternes, M. Tórtola, and J. W. F. Valle. 2020 global reassessment of the neutrino oscillation picture. *Journal of High Energy Physics*, 2021(2), Feb 2021.
- [20] A. Gando, Y. Gando, T. Hachiya, A. Hayashi, S. Hayashida, H. Ikeda, K. Inoue, K. Ishidoshiro, Y. Karino, M. Koga, and et al. Search for majorana neutrinos near the inverted mass hierarchy region with kamland-zen. *Physical Review Letters*, 117(8), Aug 2016.
- [21] P.A. Zyla et al. Ckm quark-mixing matrix. *Prog. Theor. Exp. Phys.* 2020, 2020, March 2020.

# Appendix A

## Appendix

### A.1 PMNS matrix of Majorana neutrinos in mass diagonal basis [1]

$$U_{PMNS} = \begin{pmatrix} c_{12}c_{13} & s_{13}c_{13} & s_{13}e^{-i\delta_{CP}} \\ -s_{12}c_{23} - c_{12}s_{23}s_{13}e^{i\delta_{CP}} & c_{12}c_{23} - s_{12}s_{23}s_{13}e^{i\delta_{CP}} & s_{23}c_{13} \\ s_{12}s_{23} - c_{12}c_{23}s_{13}e^{i\delta_{CP}} & -c_{12}s_{23} - s_{12}c_{23}s_{13}e^{i\delta_{CP}} & c_{23}s_{13} \end{pmatrix} \times \begin{pmatrix} e^{\frac{-i\varphi_1}{2}} & 0 & 0 \\ 0 & e^{\frac{-i\varphi_2}{2}} & 0 \\ 0 & 0 & 1 \end{pmatrix}$$

### A.2 Extended SM Lagrangians used in REAP [2][3]

$$\mathcal{L}_{MSSM+SSI} = \mathcal{L}_{MSSM} + (Y_\nu)_{ij} \mathbf{v}^{C_i} \mathbf{h}_a^{(u)} \boldsymbol{\epsilon}^{ab} \mathbf{l}_b^j \Big|_{\theta\theta} + \frac{1}{2} M_{ij} \mathbf{v}^{C_i} \mathbf{v}^{C_j} \Big|_{\theta\theta} + h.c.$$

$$\mathcal{L}_{MSSM+\kappa} = \mathcal{L}_{MSSM} - \frac{1}{4} \kappa_{ij} \mathbf{l}_a^i \boldsymbol{\epsilon}^{ab} \mathbf{h}_b^{(u)} \mathbf{l}_c^j \boldsymbol{\epsilon}^{cd} \mathbf{h}_d^{(u)} \Big|_{\theta\theta}$$

### A.3 RG running of $dim - 5$ operator ( $\kappa$ )<sup>[4]</sup>

$$16\pi^2 \frac{d\kappa}{dt} = C(Y_e^\dagger Y_e)^T \kappa + C\kappa(Y_e^\dagger Y_e) + \alpha\kappa$$

where  $\alpha_{MSSM} = -\frac{6}{5}g_1^2 - 6g_2^2 + 6(y_t^2 + y_c^2 + y_u^2)$

$$\alpha_{SM} = -3g_\tau^2 + 2(y_\mu^2 + y_e^2 + y_u^2) + 6(y_t^2 + y_b^2 + y_c^2 + y_s^2 + y_d^2 + y_u^2) + \lambda$$

$y_i$ 's are Yukawa couplings,

$g_1, g_2$  are Gauge couplings,

$\lambda$  is Higgs' Quartic coupling,

$C = 1(-\frac{3}{2})$  in MSSM (SM).

### A.4 RG running of Majorana phases<sup>[4]</sup>

$$\begin{aligned} \dot{\varphi}_1 &= \frac{Cy_\tau^2}{4\pi^2} \left\{ m_3 \cos 2\theta_{23} \frac{m_1 s_{12}^2 \sin \varphi_1 + (1 + \zeta) m_2 c_{12}^2 \sin \varphi_2}{\Delta m_{\text{atm}}^2 (1 + \zeta)} \right. \\ &\quad \left. + \frac{m_1 m_2 c_{12}^2 s_{23}^2 \sin(\varphi_1 - \varphi_2)}{\Delta m_{\text{sol}}^2} \right\} + \mathbf{O}(\theta_{13}), \\ \dot{\varphi}_2 &= \frac{Cy_\tau^2}{4\pi^2} \left\{ m_3 \cos 2\theta_{23} \frac{m_1 s_{12}^2 \sin \varphi_1 + (1 + \zeta) m_2 c_{12}^2 \sin \varphi_2}{\Delta m_{\text{atm}}^2 (1 + \zeta)} \right. \\ &\quad \left. + \frac{m_1 m_2 s_{12}^2 s_{23}^2 \sin(\varphi_1 - \varphi_2)}{\Delta m_{\text{sol}}^2} \right\} + \mathbf{O}(\theta_{13}). \end{aligned}$$

### A.5 $\alpha, \beta$ variations for $\theta_{23}, \Delta m_{\text{atm}}^2$ and $m_{\beta\beta}$ in Wolfenstein ansatz

The following tables show actual values of  $\theta_{23}, \Delta m_{\text{atm}}^2$  and  $m_{\beta\beta}$  corresponding to the symbol version tables of the same [Tables(4.1 and 4.2)].

$\alpha$	$\beta$	$\theta_{23}(\circ)$	$\Delta m_{atm}^2$	$m_{\beta\beta}$
1.0	1.0	46.3539	1.43322	2.11079
1.0	0.8	49.38	0.887399	1.67383
1.0	0.6	52.0199	0.637338	1.42275
1.0	0.4	54.2789	0.49809	1.25755
1.0	0.2	56.2207	0.40856	1.13647
0.8	1.0	41.3741	4.14956	3.94893
0.8	0.8	45.6847	1.37122	2.31377
0.8	0.6	49.4037	0.790162	1.77186
0.8	0.4	52.5181	0.551223	1.48289
0.8	0.2	55.124	0.423418	1.29696
0.6	1.0	33.4011	4.39388	4.43341
0.6	0.8	39.1744	6.25874	5.56402
0.6	0.6	44.8353	1.27487	2.58196
0.6	0.4	49.6579	0.668232	1.88884
0.6	0.2	53.4717	0.450792	1.55141
0.4	1.0	22.2035	2.08882	3.26432
0.4	0.8	27.6434	3.03408	4.27905
0.4	0.6	35.2286	23.9847	13.0667
0.4	0.4	43.6085	1.11403	2.96171
0.4	0.2	50.391	0.510454	2.03211
0.2	1.0	10.3029	3.06385	4.01182
0.2	0.8	13.1099	2.99018	4.43829
0.2	0.6	17.6549	3.50525	5.48948
0.2	0.4	26.3128	31.6739	19.3234
0.2	0.2	40.8204	0.796885	3.53775

(a) For  $\varphi_1 = 50^\circ$  and  $\varphi_2 = 0^\circ$

$\alpha$	$\beta$	$\theta_{23}(\circ)$	$\Delta m_{atm}^2$	$m_{\beta\beta}$
1.0	1.0	47.2331	1.5525	2.10196
1.0	0.8	49.0211	0.886372	1.60247
1.0	0.6	50.5051	0.615587	1.34426
1.0	0.4	51.6072	0.471114	1.18168
1.0	0.2	52.515	0.379739	1.06518
0.8	1.0	43.4824	8.72228	5.49695
0.8	0.8	46.5951	1.46966	2.29705
0.8	0.6	48.7443	0.780522	1.69121
0.8	0.4	50.3957	0.526729	1.39887
0.8	0.2	51.701	0.39572	1.21855
0.6	1.0	36.0798	2.05312	2.84405
0.6	0.8	41.3254	169.215	27.8073
0.6	0.6	45.5025	1.36636	2.56465
0.6	0.4	48.4551	0.654367	1.79926
0.6	0.2	50.5746	0.425215	1.46156
0.4	1.0	23.1005	1.22108	2.28614
0.4	0.8	29.8404	1.49939	2.80982
0.4	0.6	38.1888	6.18258	6.19802
0.4	0.4	44.3765	1.21423	2.97049
0.4	0.2	48.8965	0.495615	1.93469
0.2	1.0	9.14093	2.35076	3.04311
0.2	0.8	12.1491	2.01172	3.19063
0.2	0.6	17.6297	1.76725	3.51551
0.2	0.4	28.4644	2.66734	5.25068
0.2	0.2	42.3373	0.923916	3.66394

(b) For  $\varphi_1 = 50^\circ$  and  $\varphi_2 = 300^\circ$

Table A.1: Quantitative trends of  $\theta_{23}$ ,  $\Delta m_{atm}^2$  and  $m_{\beta\beta}$  with  $\alpha$  and  $\beta$  for  $\lambda = \lambda_{HSMU}$ . Note that  $\Delta m_{atm}^2$  is scaled by  $10^3$  and  $m_{\beta\beta}$  is scaled by 10.

$\alpha$	$\beta$	$\theta_{23}(\circ)$	$\Delta m_{atm}^2$	$m_{\beta\beta}$
1.0	1.0	54.8234	0.270761	0.945959
1.0	0.8	53.6389	0.324947	1.03312
1.0	0.6	52.1951	0.405442	1.14908
1.0	0.4	50.4061	0.536234	1.31322
1.0	0.2	48.1802	0.779898	1.56853
0.8	1.0	55.6622	0.223589	0.962148
0.8	0.8	54.467	0.271169	1.05676
0.8	0.6	52.8774	0.341779	1.18203
0.8	0.4	50.8594	0.461194	1.36506
0.8	0.2	48.2696	0.697097	1.6617
0.6	1.0	56.9483	0.17295	0.978408
0.6	0.8	55.6841	0.211174	1.0788
0.6	0.6	53.9805	0.269947	1.21617
0.6	0.4	51.7297	0.371701	1.41986
0.6	0.2	48.6096	0.588547	1.7688
0.4	1.0	58.4945	0.117817	0.993402
0.4	0.8	57.5061	0.145492	1.10021
0.4	0.6	55.8646	0.18848	1.24899
0.4	0.4	53.3675	0.265704	1.47741
0.4	0.2	49.4998	0.44454	1.89323
0.2	1.0	9.75209	0.895383	1.79708
0.2	0.8	12.7042	0.614983	1.73315
0.2	0.6	59.0013	0.0970477	1.28118
0.2	0.4	56.7985	0.14105	1.53666
0.2	0.2	52.068	0.250243	2.03366

(a) For  $\varphi_1 = 200^\circ$  and  $\varphi_2 = 300^\circ$

$\alpha$	$\beta$	$\theta_{23}(\circ)$	$\Delta m_{atm}^2$	$m_{\beta\beta}$
1.0	1.0	51.0098	0.306909	0.930683
1.0	0.8	51.3691	0.31399	0.943207
1.0	0.6	51.7609	0.321223	0.9558
1.0	0.4	52.1461	0.329536	0.969756
1.0	0.2	52.493	0.33987	0.986349
0.8	1.0	50.6015	0.297275	0.92207
0.8	0.8	50.9719	0.305505	1.03913
0.8	0.6	51.3247	0.31465	1.05746
0.8	0.4	51.6594	0.324801	1.0772
0.8	0.2	52.0149	0.335543	1.09763
0.6	1.0	50.2508	0.282858	1.14589
0.6	0.8	50.5903	0.292494	1.17032
0.6	0.6	50.906	0.303304	1.19681
0.6	0.4	51.1974	0.315315	1.22533
0.6	0.2	51.4636	0.328892	1.25649
0.4	1.0	50.014	0.258988	1.32781
0.4	0.8	50.3531	0.270136	1.36592
0.4	0.6	50.6014	0.283232	1.40859
0.4	0.4	50.7351	0.298292	1.4557
0.4	0.2	50.8837	0.315883	1.50867
0.2	1.0	50.1554	0.209777	1.62892
0.2	0.8	50.4457	0.222069	1.70121
0.2	0.6	50.3491	0.237914	1.7874
0.2	0.4	50.2614	0.25713	1.88712
0.2	0.2	50.0672	0.281961	2.00771

(b) For  $\varphi_1 = 300^\circ$  and  $\varphi_2 = 50^\circ$

Table A.2: Quantitative trends of  $\theta_{23}$ ,  $\Delta m_{atm}^2$  and  $m_{\beta\beta}$  with  $\alpha$  and  $\beta$  for  $\lambda = \lambda_{HSMU}$ . Note that  $\Delta m_{atm}^2$  is scaled by  $10^3$  and  $m_{\beta\beta}$  is scaled by 10.